

Abstract

Here we report the measurement of the comprehensive isotopic composition ($\delta^{15}\text{N}$, $\Delta^{17}\text{O}$ and $\delta^{18}\text{O}$) of nitrate at the air–snow interface at Dome C, Antarctica (DC, $75^\circ 06' \text{ S}$, $123^\circ 19' \text{ E}$) and in snow pits along a transect across the East Antarctic Ice Sheet (EAIS) between 66° S and 78° S . For each of the East Antarctic snow pits in most of which nitrate loss is observed, we derive apparent fractionation constants associated with this loss as well as asymptotic values of nitrate concentration and isotopic ratios below the photic zone. Nitrate collected from snow pits on the plateau have average apparent fractionation constants of $(-59 \pm 10)\text{‰}$, $(+2.0 \pm 1.0)\text{‰}$ and $(+8.7 \pm 2.4)\text{‰}$, for $\delta^{15}\text{N}$, $\Delta^{17}\text{O}$ and $\delta^{18}\text{O}$, respectively. In contrast, snow pits sampled on the coast show distinct isotopic signatures with average apparent fractionation constants of $(-16 \pm 14)\text{‰}$, $(-0.2 \pm 1.5)\text{‰}$ and $(+3.1 \pm 5.8)\text{‰}$, for $\delta^{15}\text{N}$, $\Delta^{17}\text{O}$ and $\delta^{18}\text{O}$, respectively. From a lab experiment carried out at DC in parallel to the field investigations, we find that the $^{15}\text{N}/^{14}\text{N}$ fractionation associated with the physical release of nitrate is $(-8.5 \pm 2.5)\text{‰}$, a value significantly different from the modelled estimate previously found for photolysis (-48‰ , Frey et al., 2009) when assuming a Rayleigh-type process. Our observations corroborate that photolysis is the dominant nitrate loss process on the East Antarctic Plateau, while on the coast the loss is less pronounced and could involve both physical release and photochemical processes. Year-round isotopic measurements at DC show a close relationship between the $\Delta^{17}\text{O}$ of atmospheric nitrate and $\Delta^{17}\text{O}$ of nitrate in skin layer snow, suggesting a photolytically-driven isotopic equilibrium imposed by nitrate recycling at this interface. The 3–4 weeks shift observed for nitrate concentration in these two compartments may be explained by the different sizes of the nitrate reservoirs and by deposition from the atmosphere to the snow. Atmospheric nitrate deposition may lead to fractionation of the nitrogen isotopes and explain the almost constant shift on the order of 25‰ between the $\delta^{15}\text{N}$ values in the atmospheric and skin layer nitrate at DC. Asymptotic $\delta^{15}\text{N}(\text{NO}_3^-)$ values and the inverse of snow accumulation rates are

Air-snow transfer of nitrate in East Antarctica – Part 1

J. Erbland et al.

Title Page

Abstract

Introduction

Conclusions

References

Tables

Figures

◀

▶

◀

▶

Back

Close

Full Screen / Esc

Printer-friendly Version

Interactive Discussion



correlated ($\ln(\delta^{15}\text{N}(\text{as.}) + 1) = (5.76 \pm 0.47) \cdot (\text{kg m}^{-2} \text{a}^{-1} / A) + (0.01 \pm 0.02)$) confirming the strong relationship between the snow accumulation rate on the residence time of nitrate in the photic zone and the degree of isotopic fractionation, consistent with previous observations by Freyer et al. (1996). Asymptotic $\Delta^{17}\text{O}(\text{NO}_3^-)$ values on the plateau are smaller compared to the values found in the skin layer most likely due to oxygen isotope exchange between the nitrate photo-products and water molecules from the surrounding ice. However, the overall fractionation in $\Delta^{17}\text{O}$ is small thus allowing the preservation of an atmospheric signal.

1 Introduction

Nitrate (NO_3^-) is the final product of the oxidation of nitrogen oxides ($\text{NO}_x = \text{NO} + \text{NO}_2$) in the atmosphere and one of the most abundant ions found in Antarctic snow (Wolff, 1995). Nitrate concentration profiles in ice cores have long been thought to preserve information regarding atmospheric NO_x sink variations and changes in the oxidative capacity of ancient atmospheres (Dibb et al., 1998). However, the stability of nitrate after deposition to the snow surface has long been questioned (Neubauer and Heumann, 1988; Mayewski and Legrand, 1990) and it is today acknowledged that its deposition is reversible at sites with low snow accumulations rates such as Dome C or Vostok on the East Antarctic Plateau (Röthlisberger et al., 2000; Blunier et al., 2005; Frey et al., 2009). The physical release of HNO_3 (via evaporation and/or desorption, often referred to as simply “evaporation”) and the photolysis of NO_3^- in the UV range (280 to 350 nm) have been proposed to explain nitrate mass loss from snow (Röthlisberger et al., 2002; Grannas et al., 2007). The relative importance of these photochemical and physical loss processes at a given site is a key issue determining the nitrate transfer function at the air–snow interface.

The effect of post-depositional processes in snow is also reflected in the stable isotopic composition of nitrate (Blunier et al., 2005; Frey et al., 2009). Stable isotope ratios in nitrate are expressed as $\delta^{15}\text{N}$, $\Delta^{17}\text{O}$ and $\delta^{18}\text{O}$ and defined as $\delta = R_{\text{spl}}/R_{\text{ref}} - 1$, with

Air-snow transfer of nitrate in East Antarctica – Part 1

J. Erbland et al.

Title Page

Abstract

Introduction

Conclusions

References

Tables

Figures

◀

▶

◀

▶

Back

Close

Full Screen / Esc

Printer-friendly Version

Interactive Discussion



R denoting the $^{15}\text{N}/^{14}\text{N}$, $^{17}\text{O}/^{16}\text{O}$ or $^{18}\text{O}/^{16}\text{O}$ isotope ratios and with the references being N_2 -AIR and VSMOW for N and O, respectively. While atmospheric particulate nitrate in non-polar atmospheres is characterized by $\delta^{15}\text{N}$ values ranging from -10% to $+10\%$ (Morin et al., 2009), extraordinarily high positive $\delta^{15}\text{N}$ values up to $+339\%$ have been observed in nitrate from the upper snowpack at Dome C and are attributed to nitrate post-depositional effects (Blunier et al., 2005; Frey et al., 2009).

Oxygen stable isotopes of nitrate provide another specific tracer, $\Delta^{17}\text{O} = \delta^{17}\text{O} - 0.52 \times \delta^{18}\text{O}$ more commonly referred to as the “oxygen isotope anomaly” or ^{17}O -excess, which quantifies the ^{17}O -excess with respect to the mass dependent fractionation rule (where $\delta^{17}\text{O} \approx 0.52 \times \delta^{18}\text{O}$). Atmospheric nitrate inherits a large positive oxygen isotopic anomaly from ozone (Michalski et al., 2003; Morin et al., 2011). Other oxidants, OH for example, possess lower $\Delta^{17}\text{O}$ values (Morin et al., 2011). Therefore, the $\Delta^{17}\text{O}$ of atmospheric nitrate is a function of the relative importance of the oxidants involved in its formation pathways and their isotopic compositions (Michalski et al., 2003; Alexander et al., 2004, 2009; Kunasek et al., 2008; Morin et al., 2008, 2009, 2011). Laboratory studies have shown a small but non-zero fractionation in $\Delta^{17}\text{O}(\text{NO}_3^-)$ due to photolysis (McCabe et al., 2005). Field observations at South Pole and Dome C confirm that the post-depositional fractionation in $\Delta^{17}\text{O}$ is minor compared to the annual signal and an atmospheric signal could likely be conserved (McCabe et al., 2007; Frey et al., 2009). Frey et al. (2009) have also suggested that nitrate oxygen stable isotopic ratios at the air–snow interface are in equilibrium; however, to this date, the transfer function of nitrate oxygen isotopes from the atmosphere to the top of the snowpack remains poorly understood.

To quantify the integrated effects of these nitrate post-depositional processes, Blunier et al. (2005) have introduced the calculation of a $^{15}\text{N}/^{14}\text{N}$ fractionation constant (denoted $^{15}\epsilon$ in their study) by applying a simple Rayleigh model which assumes a single and irreversible loss process from snow and the immediate and definitive removal of the emitted mass fraction. This approach may oversimplify the combination of processes occurring at the air–snow interface, where the nitrate reservoir may be subject

Air-snow transfer of nitrate in East Antarctica – Part 1

J. Erbland et al.

[Title Page](#)[Abstract](#)[Introduction](#)[Conclusions](#)[References](#)[Tables](#)[Figures](#)[◀](#)[▶](#)[◀](#)[▶](#)[Back](#)[Close](#)[Full Screen / Esc](#)[Printer-friendly Version](#)[Interactive Discussion](#)

to multiple loss mechanisms in addition to inputs from deposition and internal recycling (Davis et al., 2008; Frey et al., 2009). For this reason, the quantity derived by Blunier et al. (2005) shall be referred to as an “apparent” fractionation constant, which we denote $^{15}\epsilon_{\text{app}}$. In what follows, other apparent fractionation constants will be calculated: $^{17}E_{\text{app}}$ and $^{18}\epsilon_{\text{app}}$ for $\Delta^{17}\text{O}$ and $\delta^{18}\text{O}$, respectively. Note that the ϵ values are related to the commonly used fractionation factor α by $\epsilon = (\alpha - 1)$ (e.g. Criss, 1999).

Nitrogen apparent fractionation constants ($^{15}\epsilon_{\text{app}}$) calculated from Dome C snow pit profiles range from -49.8‰ to -71.0‰ (Blunier et al., 2005; Frey et al., 2009) and indicate that the nitrate fractions left in snow are enriched in ^{15}N (Blunier et al., 2005; Frey et al., 2009). A quantification of the relative importance of HNO_3 evaporation and NO_3^- photolysis at this site requires knowledge of the isotopic fractionation constants associated with each loss process. The $^{15}\text{N}/^{14}\text{N}$ fractionation associated with nitrate UV-photolysis (denoted $^{15}\epsilon_{\text{pho}}$) is calculated as follows: $^{15}\epsilon_{\text{pho}} = J'/J - 1$ with J' and J , the photolytic rate constant of $^{15}\text{NO}_3^-$ and $^{14}\text{NO}_3^-$, respectively. The photolytic rate constant is calculated as follows:

$$J = \int \Phi(\lambda, T) \sigma(\lambda, T) I(\lambda, \theta, z) d\lambda \quad (1)$$

with I , the actinic flux, Φ , the quantum yield and the absorption cross section of the considered isotopologue (σ or σ'). The absorption cross section of the less abundant isotopologue (σ') has not yet been measured; therefore it is often computed using the zero point energy shift model (Miller and Yung, 2000). Frey et al. (2009) used σ values of aqueous nitrate which had been observed for $^{14}\text{NO}_3^-$ (Chu and Anastasio, 2003) and calculated that for $^{15}\text{NO}_3^-$. Along with model estimates of I for Dome C in summer they computed an upper limit $^{15}\epsilon_{\text{pho}}$ value of -48‰ . Based on theoretical calculations, the same authors have estimated that the isotopic fractionation constant associated with the evaporation of nitrate ($^{15}\epsilon_{\text{eva}}$) should be positive, a result in contradiction with the large negative $^{15}\epsilon_{\text{app}}$ value observed in the field. This suggests that the contribution of

Air-snow transfer of nitrate in East Antarctica – Part 1

J. Erbland et al.

Title Page

Abstract

Introduction

Conclusions

References

Tables

Figures

◀

▶

◀

▶

Back

Close

Full Screen / Esc

Printer-friendly Version

Interactive Discussion



nitrate evaporation to the overall mass loss is marginal when compared to nitrate UV-photolysis (Frey et al., 2009). However, such conclusions are only based on theoretical considerations and lack experimental confirmation.

In this paper, we investigate the scale and spatial variability of photochemical and physical nitrate loss processes in East Antarctic snow. To achieve this, nitrate in shallow snow pits has been sampled in a wide area in East Antarctica. In order to derive the isotopic impact of the physical release of nitrate from snow, a nitrate “evaporation” laboratory experiment was conducted at Dome C. Isotopic fractionation constants derived from this experiment are compared to the values expected for nitrate photolysis and to apparent fractionation constants obtained in the field when available. Last, we study the isotopic transfer function of nitrate at the air–snow interface. For this purpose, the seasonal variations of the nitrate stable isotopic composition were measured at Dome C in the atmospheric particulate nitrate and in the uppermost snow layer. The data reported here together with their interpretation form the basis of a numerical model of the isotopic composition of nitrate in air and snow on ice-sheets, which is described and used in a companion paper (Erbland et al., 2012).

2 Experimental setup

2.1 Sample collection in the field

Twenty snow pits were sampled on the East Antarctic Ice Sheet between 66° S and 78° S: from D10 (a coastal location in the vicinity of the French Dumont d’Urville station in Adelie Land) to Dome C (DC, 75° 06’ S, 123° 19’ E, elevation 3233 m) and Vostok (Vk, 78° 47’ S, 106° 83’ E, elevation 3488 m) (Fig. 1). The Dome C-D10 and Dome C-Vostok transects were sampled during the austral summers 2007–2008 and 2009–2010 along the French logistical traverse and during flight operations, respectively. Additionally, two snow pits were sampled at Dome C on 26 December 2007 and 16 January 2008. Two others were collected at Vostok during the austral summer 2008–2009. In general, the

Air-snow transfer of nitrate in East Antarctica – Part 1

J. Erbland et al.

Title Page

Abstract

Introduction

Conclusions

References

Tables

Figures

◀

▶

◀

▶

Back

Close

Full Screen / Esc

Printer-friendly Version

Interactive Discussion



snow pits were sampled every two centimeters down to a depth of 20 cm to 50 cm. In some cases, one sample was taken at 90 cm depth. Nitrate mass fractions in shallow snow pits can be as low as 10 ng g^{-1} (Frey et al., 2009); therefore, for each sample, approximately 1 kg of snow was collected in a 2-l sealed plastic bag which secured the collection of an adequate amount of nitrate for the isotopic analysis (100 nmol per analysis, Morin et al., 2009) and reruns, if necessary.

Air and surface snow sampling were carried out at Dome C from January 2009 to January 2010. The first 3–4 mm of the non-cohesive surface snow, referred to as the “skin layer”, was collected approximately every three days throughout the campaign. Additionally, a 30-h intensive hourly collection campaign was conducted on 28–29 December 2009. Approximately 300 grams of skin layer snow were collected for each skin layer sample in 1 l sealed plastic bags (nitrate mass fractions can be smaller than 100 ng g^{-1}). Atmospheric samples were collected at DC during the same time period on glass fiber filters ($20.3 \text{ cm} \times 25.4 \text{ cm}$) using a high-volume air sampler (HVAS) which has been used during previous campaigns and has been shown to quantitatively trap both particulate nitrate and gaseous HNO_3 (Frey et al., 2009). Samples were collected for 37 separate 5–7 day periods at an average flow rate of $1 \text{ m}^3 \text{ min}^{-1}$ (STP, $T = 273.15 \text{ K}$ and $P = 1013 \text{ hPa}$), which was necessary to ensure the collection of a sufficient amount of nitrate for isotopic analysis (atmospheric concentrations can be as low as 1 ng m^{-3}). Filters were then removed from the HVAS and placed into clean 50 cm^3 centrifuge tubes, put in sealed plastic bags and stored at -20°C .

2.2 “Nitrate evaporation” experiment

An experiment was conducted at Dome C during the summer campaign 2009–2010 to test the impact of the physical release of nitrate on its isotopic composition. Briefly, surface snow highly concentrated in nitrate (first top mm) was collected on 21 December 2009, homogenized and equally distributed into 4-cm thick layers on three rectangular plates ($40 \text{ cm} \times 20 \text{ cm}$, 600 g on each plate). Each plate was stored in the dark and in three different closed rooms with temperatures of -10°C , -20°C and

28565

Air-snow transfer of nitrate in East Antarctica – Part 1

J. Erbland et al.

Title Page

Abstract

Introduction

Conclusions

References

Tables

Figures

⏪

⏩

◀

▶

Back

Close

Full Screen / Esc

Printer-friendly Version

Interactive Discussion



–30 °C, respectively. The temperature in each room was controlled using an electrical heater and was measured every two days. Average temperatures were (-10.4 ± 1.3) °C, (-21.6 ± 3.8) °C and (-31.4 ± 1.3) °C (mean $\pm 1\sigma$), respectively. For the sake of simplicity, in the following, we prefer to denote the experiments using their target temperatures (i.e. –10 °C, –20 °C and –30 °C). The snow was sub-sampled in 1-l sealed plastic bags over a two-week period and at a two-day resolution. Snow mass was regularly measured to monitor sublimation.

2.3 Chemical and isotopic analysis

All snow samples (skin layer, snow pit and samples from the evaporation experiment) were pre-processed in the field except those from the two pits collected at Vostok in 2008–2009, which were double-sealed in plastic bags and shipped to France, where they were pre-processed in our laboratory. Each sample was melted at room temperature and NO_3^- concentrations were determined from an aliquot using a colorimetric method employed routinely at DC (Frey et al., 2009). From nitrate concentrations measured in the melted snow samples, we derive nitrate mass fractions expressed in ngg^{-1} and denoted $w(\text{NO}_3^-)$ in the following. Nitrate mass fractions retrieved from each evaporation experiment sample were corrected for snow sublimation. Nitrate ions in the remaining melted sample were then concentrated on 0.3 cm^3 of an anionic exchange resin (BioRad™ AG 1-X8, chloride form) and subsequently eluted with $5 \times 2 \text{ cm}^3$ of a NaCl 1 M solution allowing for a 100 % recovery (Silva et al., 2000; Frey et al., 2009).

Atmospheric nitrate collected on the glass filters was quantitatively extracted in 40 cm^3 of ultra-pure water via centrifugation using Millipore Centricon™ filter units. Nitrate concentrations were then determined using the same colorimetric method as described above. Atmospheric nitrate concentrations are further denoted $\gamma(\text{NO}_3^-)$ and were calculated as the ratio of the total NO_3^- filter loading and the total volume of air pumped through the filter at STP conditions.

Air-snow transfer of nitrate in East Antarctica – Part 1

J. Erbland et al.

Title Page

Abstract

Introduction

Conclusions

References

Tables

Figures

◀

▶

◀

▶

Back

Close

Full Screen / Esc

Printer-friendly Version

Interactive Discussion



Isotope ratios of NO_3^- ($^{15}\text{N}/^{14}\text{N}$, $^{17}\text{O}/^{16}\text{O}$ and $^{18}\text{O}/^{16}\text{O}$) were measured on a Thermo FinniganTM MAT 253 isotope ratio mass spectrometer, equipped with a GasBench IITM and coupled to an in-house built nitrate interface (Morin et al., 2009). Briefly, denitrifying bacteria *Pseudomonas Aureofaciens* convert NO_3^- in N_2O in anaerobic conditions (Sigman et al., 2001; Casciotti et al., 2002). N_2O is then thermally decomposed on a gold surface heated to 900°C producing a mixture of O_2 and N_2 which is then separated by gas chromatography (Kaiser et al., 2007) and injected into the mass spectrometer for the dual O and N analysis (Morin et al., 2009).

Isotopic data were corrected for any isotopic effect occurring during the analytical procedure by using the same approach as Morin et al. (2009) and Frey et al. (2009): international reference materials (IAEA USGS-32, 34 and 35) were prepared in an identical way and followed the same analytical procedures. This identical treatment includes the use of the same background matrix (ultrapure water and NaCl 1M solution for atmospheric and snow samples, respectively) as well as the same water isotopic composition for the standards and samples. For each batch of 60 samples, the overall accuracy of the method is estimated as the reduced standard deviation of the residuals from the linear regression between the measured reference materials ($n = 16$) and their expected values. For the snow results described here (230 samples in total), the average uncertainty values obtained for $\delta^{18}\text{O}$, $\Delta^{17}\text{O}$ and $\delta^{15}\text{N}$ were 2.3‰, 0.4‰ and 0.5‰, respectively while they are 1.6‰, 0.5‰ and 1.0‰ for the 37 atmospheric analysis.

2.4 Data reduction and complementary data

The $^{15}\text{N}/^{14}\text{N}$ fractionation constant associated with each evaporation experiment (denoted $^{15}\epsilon_{\text{eva}}$) has been calculated following Blunier et al. (2005)'s approach which assumes a Rayleigh-type single loss process with irreversible removal of nitrate from the snow. Blunier et al. (2005)'s formulation for $^{15}\epsilon$ can be extended to $^{18}\epsilon$ and ^{17}E .

Air-snow transfer of nitrate in East Antarctica – Part 1

J. Erbland et al.

Title Page

Abstract

Introduction

Conclusions

References

Tables

Figures

◀

▶

◀

▶

Back

Close

Full Screen / Esc

Printer-friendly Version

Interactive Discussion



Basically, ${}^n\epsilon$ ($n = 15, 17$ or 18) is calculated as the slope of the best linear regression of data in the $\ln(1 + \delta^n(\text{NO}_3^-))$ versus $(\ln(w(\text{as.}))/\text{ng g}^{-1})$ space.

The large amount of isotopic data obtained for snow across East Antarctica has been reduced in two ways. First, apparent fractionation constants were calculated using Blunier et al. (2005)'s approach explicated in the above paragraph. The isotopic fractionation constants derived from these snow pit data are therefore termed "apparent" (and subscripted "app") because they represent the integrated isotopic effect of the processes involving nitrate in the top decimeters of the snowpack and in the lower atmosphere.

Second, asymptotic values were calculated for each snow pit. In the following, the asymptotic value of the quantity X ($= w(\text{NO}_3^-)$, $\delta^{15}\text{N}$, $\Delta^{17}\text{O}$ and $\delta^{18}\text{O}$) is denoted $X(\text{as.})$ and was calculated assuming an exponential behaviour of X with depth (z) as expressed in Eq. (2):

$$X(z) = X(\text{as.}) + [X(0) - X(\text{as.})]e^{-z/\eta(X)} \quad (2)$$

with $\eta(X)$, the decay parameter specific to the quantity X , which is varied in the 1–30 cm range and at a 1 cm resolution. Data from each snow pit were fitted using the above equation and the best set of parameters $[X(0), X(\text{as.}), \eta(X)]$ was determined by minimizing the sum of squared residuals. For each snow pit, 1- σ uncertainty in the asymptotic quantity X was estimated by calculating the standard deviation of the residuals. Given the above definition of $w(\text{as.})$, $\delta^{15}\text{N}(\text{as.})$, $\Delta^{17}\text{O}(\text{as.})$ and $\delta^{18}\text{O}(\text{as.})$, these terms represent the asymptotic mass fraction and isotopic composition reached by nitrate below the zone of active nitrate mass loss in the top decimeters of snow. In the case of photolysis, this zone is termed the "photic zone" and its lower limit represents the depth at which the actinic flux is mostly null. Radiative transfer in snow depends on e-folding depth (Simpson et al., 2002; Domine et al., 2008), which has been observed to be on the order of 10 cm in the top snowpack layers at Dome C and for wavelengths in the 350 nm to 400 nm range (France et al., 2011). Thus, in the case of plateau sites such as DC, the photic zone has a thickness on the order of 30 cm because 95 % of

Air-snow transfer of nitrate in East Antarctica – Part 1

J. Erbland et al.

Title Page

Abstract

Introduction

Conclusions

References

Tables

Figures

◀

▶

◀

▶

Back

Close

Full Screen / Esc

Printer-friendly Version

Interactive Discussion



the UV radiation is lost below this depth. Therefore, the asymptotic values derived in this study represent nitrate well below the photic zone, i.e. nitrate which can be considered inert with respect to photo-processes.

Snow accumulation rates and mean annual temperatures are denoted A and T_a , respectively. For the DC and Vostok sites, A and T_a have been obtained from EPICA community members (2004) and Ekaykin et al. (2002), respectively. For the other 15 East Antarctic sites, A and T_a have been interpolated from 1980–2007 simulations of the atmospheric circulation model LMDZ4 (Krinner et al., 2007) and derived from the ERA-Interim reanalysis over the 2000–2008 period (Dee et al., 2011), respectively. The snow accumulation rates, assumed to be stationary in time, is used for the calculation of the asymptotic nitrate mass flux denoted $F(\text{as.})$, expressed in $\text{kg m}^{-2} \text{a}^{-1}$ (N equivalent) and calculated as $F(\text{as.}) = \frac{m_{\text{N}}}{m_{\text{NO}_3^-}} \times w(\text{as.}) \times A$, with $w(\text{as.})$ in NO_3^- equivalent.

3 Results

3.1 Upper snowpack profiles of NO_3^- in East Antarctica

Figures 2 and 3 show the nitrate mass fraction and isotopic composition ($\delta^{15}\text{N}$ and $\Delta^{17}\text{O}$) in each of the 20 snow pits sampled in this study. NO_3^- mass fraction profiles in each snow pit show a decreasing trend over the uppermost 1–2 dm of snow. The decrease is moderate (around 50 %) at sites close to D10 and dramatic on the plateau, at Dome C, Vostok and sites in between those locations. For example, every snow pit sampled at DC shows nitrate mass fractions reduced by 80 % in the top 10 cm (panel 13 on Fig. 2), which is consistent with all previous observations (Röthlisberger et al., 2000; Blunier et al., 2005; Frey et al., 2009).

A similar spatial variability is also observed for $\delta^{15}\text{N}$ (Fig. 2) with values increasing by 250 ‰ (to values as high as +359.7 ‰ in the S4 pit) over the top 50 cm of snow on the plateau while a weak increase of 10 ‰ is observed on the coast. The same applies for $\delta^{18}\text{O}$, with the lowermost value found in the S3 pit (+10.9 ‰) (data not

Air-snow transfer of nitrate in East Antarctica – Part 1

J. Erbland et al.

Title Page

Abstract

Introduction

Conclusions

References

Tables

Figures

◀

▶

◀

▶

Back

Close

Full Screen / Esc

Printer-friendly Version

Interactive Discussion



shown here but provided in Fig. 20, Supplement). The high enrichment in $\delta^{15}\text{N}$ and depletion in $\delta^{18}\text{O}$ observed at the Dome C site (up to +250‰ and +30‰, respectively) are consistent with previous studies (Blunier et al., 2005; Frey et al., 2009). The ^{17}O -excess in surface snow nitrate varies between 23‰ and 38‰. On the East Antarctic Plateau, the $\Delta^{17}\text{O}$ values in nitrate of the upper snow layers are on the order of 30‰ and decrease to 20–25‰ at 50 cm depth. Some $\Delta^{17}\text{O}(\text{NO}_3^-)$ profiles at plateau sites show oscillations with amplitudes of 5–7‰ (e.g. snow pit S2, Panel 15 on Fig. 3 or Fig. 19 in Supplement), consistent with previous observations by Frey et al. (2009) at DC. At such low accumulation sites, $\Delta^{17}\text{O}(\text{NO}_3^-)$ also shows a decreasing trend with depth with a reduction of up to 10‰.

Figure 4 presents an example of the data reduction procedure used to derive the asymptotic values in the case of snow pit S4 sampled at Vostok (Eq. 2). The other snow pits together with the related exponential fits are individually displayed in the Supplement. Figures 5–7 and Table 1 present the reduced data together with the data previously published for Dome C (“DC03”, Blunier et al., 2005, “DC04” and “DC07–1”, Frey et al., 2009). The uncertainty derived for the asymptotic values are small in most cases (Table 1 and Fig. 6a–c). Values of the asymptotic isotopic ratios show significant spatial gradients across East Antarctica (Fig. 6a–c, respectively): in comparison to values found close to the coast, $\delta^{18}\text{O}(\text{as.})$ and $\Delta^{17}\text{O}(\text{as.})$ are lower by more than 80‰ and 20‰, respectively and $\delta^{15}\text{N}(\text{as.})$ is higher by more than 300‰ at Vostok. Values of asymptotic nitrate mass fractions also show a spatial variability with lower concentrations on the plateau ($w(\text{as.})$ values generally below 50 ng g^{-1}) than on the coast (values up to 120 ng g^{-1}) (Fig. 7a). The asymptotic nitrate flux is an order of magnitude lower on the plateau ($F(\text{as.}) < 1\text{ mg m}^{-1}\text{ a}^{-1}$, N equivalent) than at D10.

Figure 5a–c as well as Table 1 present the apparent isotopic fractionation constants derived for each snow pit. Apparent isotopic fractionation constants obtained for DC in this study range from +6.1‰ to +9.4‰ for $^{18}\epsilon_{\text{app}}$, from +1.2‰ to +1.7‰ for $^{17}E_{\text{app}}$ and from –72.7‰ to –40.0‰ for $^{15}\epsilon_{\text{app}}$, and are within the range of previous observations at this site (Fig. 5 and Table 1).

Air-snow transfer of nitrate in East Antarctica – Part 1

J. Erbland et al.

[Title Page](#)[Abstract](#)[Introduction](#)[Conclusions](#)[References](#)[Tables](#)[Figures](#)[◀](#)[▶](#)[◀](#)[▶](#)[Back](#)[Close](#)[Full Screen / Esc](#)[Printer-friendly Version](#)[Interactive Discussion](#)

3.2 $^{15}\text{N}/^{14}\text{N}$ fractionation associated with nitrate evaporation

Figure 8 shows the results of the HNO_3 evaporation experiment carried out at DC in parallel to the field observations. The initial snow had a nitrate mass fraction of 1471 ng g^{-1} and $\delta^{15}\text{N}$ value of $+28.1\text{‰}$, which are typical values for the skin layer at DC. Table 2 gives the total nitrate and snow mass fractions lost at the end of each experiment. The minimum nitrate and snow mass losses (10 % and 1 %) are observed for the experiment conducted at -30°C . On the other hand, the maximum nitrate and snow mass losses (40 % and 72 %) are observed for the experiment conducted at -10°C , although this experiment was four days shorter than the two others.

$\delta^{15}\text{N}$ in snow nitrate of the -30°C and -20°C experiments remained constant with averages ($\pm 1\text{-}\sigma$) of $(27.5 \pm 0.2)\text{‰}$ and $(27.6 \pm 0.4)\text{‰}$, respectively. However, nitrate in the -10°C experiment was 4.2‰ higher after 10 days. The -30°C and -20°C experiments yield $^{15}\text{N}/^{14}\text{N}$ fractionation constants not significantly different from zero ($^{15}\epsilon_{\text{eva}}$ values of $(+1.8 \pm 3.0)\text{‰}$ and $(+0.6 \pm 1.8)\text{‰}$, respectively) while the -10°C experiment is associated with a $^{15}\epsilon_{\text{eva}}$ value which is significantly negative: $(-8.5 \pm 2.5)\text{‰}$ (Table 2).

3.3 Annual atmospheric and skin layer variations at Dome C

3.3.1 Annual cycle of NO_3^- concentrations

Figure 9b shows the atmospheric and skin layer nitrate concentrations observed at Dome C during 2009–2010. Atmospheric NO_3^- concentrations remained relatively low and steady for most of the year, with an average value of $(5.9 \pm 4.1) \text{ ng m}^{-3}$ during the polar night period, i.e. from March to September 2009. Sporadic concentration maxima greater than $> 90 \text{ ng m}^{-3}$ occurred in spring, concurrently with the return of continuous sunlight at DC (see UV-B* dose in Fig. 9a). During this period of maximum photochemical activity (October to December), NO_3^- concentrations reached an average value of $(61.9 \pm 19.2) \text{ ng m}^{-3}$, then decreased sharply to values lower than 30 ng m^{-3} in early

summer (January 2010), in agreement with previous observations at DC in 2007 (Frey et al., 2009) and at South Pole in 2004 (McCabe et al., 2006).

NO_3^- mass fractions in the skin layer snow exhibit a seasonal pattern similar to that observed for the atmosphere: low and steady mass fractions, $(161 \pm 50) \text{ ng g}^{-1}$, are observed during polar night, followed by a sharp increase to values in the 600–1400 ng g^{-1} range in the spring and early summer, consistent with previous results obtained for daily surface snow samples at Halley, Antarctica (Wolff et al., 2008). Temporal variations of NO_3^- mass in the skin layer are offset from those observed in the atmosphere by a period of approximately 3–4 weeks. For instance, while atmospheric NO_3^- concentration increases above its background level in mid-October, skin layer NO_3^- mass fraction does not begin to increase until mid-November.

3.3.2 Annual cycle of nitrate isotopic composition

Figures 9c and 10b show the annual variations of the atmospheric and skin layer $\delta^{15}\text{N}(\text{NO}_3^-)$ and $\Delta^{17}\text{O}(\text{NO}_3^-)$ at DC in 2009–2010 and are further described below.

$\delta^{15}\text{N}(\text{NO}_3^-)$ shows the same features as those reported in 2007–2008 by Frey et al. (2009): from March to August, $\delta^{15}\text{N}$ in atmospheric nitrate fluctuates between -14.0‰ and $+12.8\text{‰}$ with a mean value of $(1.6 \pm 6.5)\text{‰}$. Along with the increase of surface temperatures and UV radiation, $\delta^{15}\text{N}(\text{NO}_3^-)$ gradually decreases to reach its lowest value (-30.8‰ compared to -35.0‰ for Frey et al., 2009) in mid-October. The annual weighted $\delta^{15}\text{N}$ value is -6.5‰ . In the skin layer, $\delta^{15}\text{N}(\text{NO}_3^-)$ has an annual weighted mean of $+18.2\text{‰}$. The lowest values (-11.7‰) are found in spring, by the end of October. After this minimum, $\delta^{15}\text{N}$ steadily increases to reach values above $+30\text{‰}$ by the end of the summer. While the polar night is characterized by a skin layer snow featuring $\delta^{15}\text{N}$ values of $(21.1 \pm 7.7)\text{‰}$, drastic variations of more than 40‰ can be observed between two consecutive samples. On average, $\delta^{15}\text{N}$ in the skin layer nitrate is on the order of 25‰ higher than $\delta^{15}\text{N}$ in the atmospheric nitrate.

Air-snow transfer of nitrate in East Antarctica – Part 1

J. Erbland et al.

Title Page

Abstract

Introduction

Conclusions

References

Tables

Figures

◀

▶

◀

▶

Back

Close

Full Screen / Esc

Printer-friendly Version

Interactive Discussion



$\Delta^{17}\text{O}$ for the atmospheric nitrate sampled at Dome C in 2009–2010 is consistent with previous measurements in 2007–2008: the highest values ($> 40\text{‰}$) are observed during August while the signal flattens in summer to reach its lowermost values (around 29‰ , Frey et al., 2009). $\Delta^{17}\text{O}$ in skin layer nitrate displays a similar trend but with less variations and an average shift of a few ‰ (Fig. 10b). Indeed, the annual mass weighted $\Delta^{17}\text{O}$ averages calculated for the atmospheric and skin layer nitrate are 29.4‰ and 31.7‰ , respectively.

3.4 Intensive skin layer collection at Dome C

Results of the 30-h intensive skin layer collection carried out at Dome C are given in Fig. 11. Between 28 December and 29 December 2009, nitrate in the skin layer snow at Dome C show average ($\pm 1\sigma$) mass fraction, $\delta^{15}\text{N}$, $\Delta^{17}\text{O}$ and $\delta^{18}\text{O}$ values of $(1261 \pm 105) \text{ ngg}^{-1}$, $(17.0 \pm 1.0)\text{‰}$, $(28.6 \pm 1.2)\text{‰}$ and $(56.2 \pm 3.6)\text{‰}$, respectively consistent with the annual data obtained for this period and shown in Figs. 9 and 10.

Data obtained for the 30-h intensive skin layer collection at Dome C show small scatters in the isotopic ratios in skin layer nitrate (1.0‰ , 1.2‰ and 3.6‰ for $\delta^{15}\text{N}$, $\Delta^{17}\text{O}$ and $\delta^{18}\text{O}$, respectively) which are very close to the analytical errors obtained for those samples (0.9‰ , 1.0‰ and 2.3‰ , respectively). Hence, the observed small variations in $\delta^{15}\text{N}$ and $\Delta^{17}\text{O}$ in hourly skin layer nitrate collections are not quantitatively significant. The chosen sampling method (i.e. one skin layer sample collection every 3 days on average) is therefore appropriate to track annual variations in the isotopic composition of nitrate in this reservoir.

Air-snow transfer of nitrate in East Antarctica – Part 1

J. Erbland et al.

[Title Page](#)[Abstract](#)[Introduction](#)[Conclusions](#)[References](#)[Tables](#)[Figures](#)[⏪](#)[⏩](#)[◀](#)[▶](#)[Back](#)[Close](#)[Full Screen / Esc](#)[Printer-friendly Version](#)[Interactive Discussion](#)

4 Discussion

4.1 Relative contribution of nitrate post-depositional processes in East Antarctica

4.1.1 Process-specific $^{15}\text{N}/^{14}\text{N}$ fractionation constants

5 The results of the nitrate evaporation experiments conducted in this study show that this process may be associated with a $^{15}\text{N}/^{14}\text{N}$ fractionation constant near zero, thus significantly different from the expected value for UV-photolysis. The $^{15}\epsilon_{\text{eva}}$ value derived from the experiment conducted at -10°C is negative (-8.5‰ , Table 2) indicating that the remaining snow is enriched in ^{15}N . This value is much less negative than the $^{15}\epsilon$ value for photolysis in DC conditions (-48‰ , Frey et al., 2009). The $^{15}\epsilon_{\text{eva}}$ values derived from the -30°C and -20°C experiments are not significantly different from zero, which seems to be linked to the small nitrate mass loss obtained after 14 days for these two experiments conducted at low temperatures (1 % and 7 % for the -30°C and -20°C experiments, respectively, to compare to 40 % at -10°C and after 10 days).
15 The different temperatures used in this experiment must not be seen as relevant for different Antarctic sites conditions but rather as a way to force nitrate mobility through snow metamorphism. Not all the conditions were controlled during the three different evaporation experiments. Indeed, it is possible that atmospheric HNO_3 deposition was not prevented in our setup. However, we believe that this process should be limited
20 given that all of the experiments were conducted in closed spaces where atmospheric HNO_3 is more likely to stick on walls rather than on snow. This is further supported by the experiments conducted at -20°C and -30°C where no nitrate gain was observed. Our results therefore clearly show that the evaporation of nitrate is associated with an isotopic fractionation constant close to zero (-8.5‰) thus different from the
25 $^{15}\epsilon_{\text{app}}$ values measured at Dome C (as low as -71.0‰ , Frey et al., 2009). Therefore, the dominant contribution of one of these two processes will be possible on the basis of the comparison of $^{15}\epsilon_{\text{app}}$ values to $^{15}\epsilon_{\text{pho}}$ and $^{15}\epsilon_{\text{eva}}$.

Air-snow transfer of nitrate in East Antarctica – Part 1

J. Erbland et al.

Title Page

Abstract

Introduction

Conclusions

References

Tables

Figures

◀

▶

◀

▶

Back

Close

Full Screen / Esc

Printer-friendly Version

Interactive Discussion



Air-snow transfer of nitrate in East Antarctica – Part 1

J. Erbland et al.

Title Page

Abstract

Introduction

Conclusions

References

Tables

Figures

⏪

⏩

◀

▶

Back

Close

Full Screen / Esc

Printer-friendly Version

Interactive Discussion

Moreover, the low dynamics observed over 14 days in the “evaporation” experiments conducted at -30°C and -20°C contrast with the high variation found in mass fraction of the skin layer nitrate at Dome C (Fig. 9b). Therefore, a loss process faster than nitrate evaporation is necessary to explain the high variations in skin layer nitrate mass fraction at DC. We also note that some drastic changes in skin layer nitrate mass fractions between two consecutive samples could be linked to uncertainty in sampling depth as well as enhanced nitrate deposition through the precipitation of diamond dust. Indeed, sampling more than the 3–4 mm target will cause an apparent decrease in nitrate mass fraction such as the one observed on 28 December 2009 at 10:00 (Fig. 11a).

A great advantage of this experiment is its use of natural snow as opposed to previous laboratory experiments (e.g. McCabe et al., 2005). Despite its uncertainties, the present experiment does not support that the loss could be dominated by direct re-emission of HNO_3 or snow metamorphism at Dome C.

4.1.2 Dominant loss process on the plateau and the coast

In what follows, the East Antarctic Ice Sheet is divided into three zones with respect to the observed $^{15}\epsilon_{\text{app}}$, $^{18}\epsilon_{\text{app}}$ and $^{17}E_{\text{app}}$ values: the coast (features $A > 200 \text{ kg m}^{-2} \text{ a}^{-1}$, $T_a > -35^{\circ}\text{C}$ and elev. $< 2500 \text{ m}$), the plateau (features $A < 50 \text{ kg m}^{-2} \text{ a}^{-1}$, $T_a \leq -45^{\circ}\text{C}$ and elev. $> 3150 \text{ m}$) (Fig. 1) and a transition zone between the two. Along the D10–DC and DC–Vostok transects presented in this study, sites in the coastal zone are within 400 km to D10 and beyond 1100 km to D10 for sites in the plateau zone. The coast, transition and plateau zones contain five, five and seven sites, respectively. Table 3 presents the average, standard deviation and minimum and maximum values for each apparent fractionation constant calculated for the coastal and plateau zones. Plateau sites are characterized by a low average $^{15}\epsilon_{\text{app}}$ value ($(-59 \pm 10)\text{‰}$), and average $^{18}\epsilon_{\text{app}}$ and $^{17}E_{\text{app}}$ values of $(+8.7 \pm 2.4)\text{‰}$ and $(+2.0 \pm 1.0)\text{‰}$, respectively. In contrast, coastal sites are characterized by a moderate $^{15}\text{N}/^{14}\text{N}$ apparent fractionation constant,

(-16 ± 14)‰ on average, and $^{18}\epsilon_{\text{app}}$ and $^{17}E_{\text{app}}$ values which are insignificantly different from zero: ($+3.1 \pm 5.8$)‰ and (-0.2 ± 1.5)‰, respectively.

Uncertainties in the calculation of the apparent fractionation constants for individual snow pits reveal the degree to which the assumed single-step Rayleigh model is reasonable in explaining the observed isotopic features at depth. On the plateau and on the coast, the uncertainties are small as shown in Fig. 5a, b and c and in Table 1. This observation suggests that the single-step Rayleigh fractionation model assumed for the calculation of $^{15}\epsilon_{\text{app}}$, $^{18}\epsilon_{\text{app}}$ and $^{17}E_{\text{app}}$ is used appropriately and indicates that nitrate loss from snow is governed by a single process in these zones. In contrast, uncertainties are large for sites in the transition zone where nitrate mass loss from snow may be due to a combination of multiple loss processes.

Nitrate UV-photolysis and evaporation have competitive isotopic effects given their two distinct $^{15}\epsilon$ signatures. As discussed above, the use of an apparent fractionation constant allows for the quantification of the integrated isotopic effect of nitrate post-depositional processing in the upper snow and lower atmosphere. At this interface, nitrogen isotopes of nitrate may undergo fractionation through other processes such as local recycling from the re-deposition of either re-oxidized photochemical products or directly emitted HNO_3 . In what follows, we neglect any possible $^{15}\text{N}/^{14}\text{N}$ fractionation due to re-oxidation and redeposition because the difference they may cause at the air-snow interface (on the order of 25‰ on average at DC) is small when compared to the enrichments of more than +200‰ which are observed in the snow profiles. Under this assumption, $^{15}\epsilon_{\text{eva}}$ and $^{15}\epsilon_{\text{pho}}$ can be directly compared to $^{15}\epsilon_{\text{app}}$ to determine the relative importance of the two loss processes. Therefore, in the extreme case, where the UV-photolysis dominates the mass loss, $^{15}\epsilon_{\text{app}}$ values derived from snow pits must be close to $^{15}\epsilon_{\text{pho}}$.

On the plateau, the average $^{15}\epsilon_{\text{app}}$ is (-59 ± 10)‰ (Table 3), a value close to an estimate of $^{15}\epsilon_{\text{pho}}$ based on a photolytic fractionation model and DC radiation conditions for summer solstice (< -48 ‰, Frey et al., 2009). This average $^{15}\epsilon_{\text{app}}$ value is

Air-snow transfer of nitrate in East Antarctica – Part 1

J. Erbland et al.

[Title Page](#)[Abstract](#)[Introduction](#)[Conclusions](#)[References](#)[Tables](#)[Figures](#)[⏪](#)[⏩](#)[◀](#)[▶](#)[Back](#)[Close](#)[Full Screen / Esc](#)[Printer-friendly Version](#)[Interactive Discussion](#)

characteristic of the plateau zone, given the small standard deviation associated with it. From this, we conclude that nitrate UV-photolysis not only dominates the nitrate $^{15}\text{N}/^{14}\text{N}$ fractionation but also the nitrate mass loss on the plateau. In this zone, nitrate evaporation therefore leads to only a minor net mass loss but it is nevertheless possible that evaporation is responsible for nitrate mobility within the snowpack, at the macroscopic scale, under the effect of H_2O mobility for example (Pinzer et al., 2012). The positive and significant average $^{17}E_{\text{app}}$ and $^{18}\epsilon_{\text{app}}$ values observed on the plateau, $(+2.0 \pm 1.0)\text{‰}$ and $(+8.7 \pm 2.4)\text{‰}$ (Table 3), are consistent with a dominant nitrate UV-photolysis because they reflect the fact that a fraction of the photoproducts undergo an isotopic exchange with a source of O atoms featuring low $\delta^{18}\text{O}$ and $\Delta^{17}\text{O}$ values (such as H_2O molecules of snow, McCabe et al., 2005). Figures 5b and 7c further show that $^{17}E_{\text{app}}$ is weakly sensitive to the local annual average temperature for East Antarctic Plateau sites. Cage recombination effects of nitrate photo-products may therefore be rather insensitive to temperature variations in the -55°C to -47°C range. This result could be highly relevant for the analysis of the $\Delta^{17}\text{O}$ profiles of nitrate trapped in deep ice cores retrieved from plateau sites such as Dome C or Vostok.

In contrast, coastal sites are characterized by a moderate average $^{15}\text{N}/^{14}\text{N}$ fractionation, $(-16 \pm 14)\text{‰}$, and average oxygen isotopic fractionation constants not significantly different from zero: $(+3.1 \pm 5.8)\text{‰}$ and $(-0.2 \pm 1.5)\text{‰}$ for $^{18}\epsilon_{\text{app}}$ and $^{17}E_{\text{app}}$, respectively. In this zone, the observed nitrate mass loss rates are small (Fig. 2) and a precise discussion of the relative contribution of the physical and photochemical loss processes remains delicate. We however observe that the average $^{15}\epsilon_{\text{app}}$ value observed on the coast is closer to the experimental $^{15}\epsilon_{\text{eva}}$ value than to the modelled $^{15}\epsilon_{\text{pho}}$ value, which suggests that the physical release of nitrate is a greater contributor to nitrate mass loss from snow than UV-photolysis in this area. This conclusion is further supported by the observation of average $^{17}E_{\text{app}}$ and $^{18}\epsilon_{\text{app}}$ values not significantly different from zero in this zone, which suggests an absence of oxygen isotope exchange. On the coast, the physical release of nitrate is likely encouraged by the high air temperatures combined with the high wind speeds which are prevalent in this area (Gallet et al., 2011). In

Air-snow transfer of nitrate in East Antarctica – Part 1

J. Erbland et al.

Title Page

Abstract

Introduction

Conclusions

References

Tables

Figures

◀

▶

◀

▶

Back

Close

Full Screen / Esc

Printer-friendly Version

Interactive Discussion



contrast, we note that the high snow accumulation rates featuring coastal sites cannot explain the greater contribution of the physical release of nitrate to the total observed mass loss since this variable would equally act on the two loss processes by limiting nitrate residence time in the zone of active loss (the photic zone when considering photolysis).

Last, the transition zone between the coast and the plateau shows $^{15}\epsilon_{\text{app}}$ values which vary well within the average values observed for the two extreme geographic zones indicating a transition from a “coastal” to a “plateau” regime. This transition zone appears to host a combination of nitrate loss processes.

4.2 Dynamic equilibrium at the air–snow interface at Dome C?

The fact that nitrate UV-photolysis dominates the mass loss from snow on the plateau has important implications in terms of local N cycling. Given the short photochemical lifetimes of NO_x and HNO_3 above the plateau during summer (approx. 15 h, Davis et al., 2008 and 3.5 h, Huey et al., 2004, respectively for South Pole conditions), the release of NO_x through nitrate UV-photolysis initiates a complex and rapid local recycling of nitrogen at the air–snow interface (Davis et al., 2008; Morin et al., 2009; Frey et al., 2009). This rapid recycling (loss, oxidation, deposition) may result in an equilibrium between atmospheric and surface snow nitrate as previously suggested by Frey et al. (2009). Here we test this hypothesis in light of our observations at the air–snow interface at Dome C.

Nitrate photolysis occurring during summer may explain the average 25‰ enrichment observed in $\delta^{15}\text{N}$ in snow versus the atmospheric nitrate at Dome C. Indeed, the negative $^{15}\text{N}/^{14}\text{N}$ fractionation constant modelled for UV-photolysis ($^{15}\epsilon_{\text{pho}} = -48\%$ Frey et al., 2009) means that the emitted N mass fraction is depleted in ^{15}N (Savarino et al., 2007; Morin et al., 2009; Frey et al., 2009) as observed for atmospheric nitrate in spring and summer (Fig. 9c). As a first order estimate, the photolytically produced NO_x should be depleted by 48‰ compared to the initial nitrate in snow. Such an important

Air-snow transfer of nitrate in East Antarctica – Part 1

J. Erbland et al.

Title Page

Abstract

Introduction

Conclusions

References

Tables

Figures

◀

▶

◀

▶

Back

Close

Full Screen / Esc

Printer-friendly Version

Interactive Discussion



5 difference is not observed between the atmosphere and the skin layer. One possible explanation for this involves the snow layers directly below the skin layer, which may also participate in NO_x production. These deeper layers contain nitrate which displays increasing $\delta^{15}\text{N}$ values with increasing depth (Panel 13 on Fig. 2). Therefore, the NO_x produced from these layers also have increasing $\delta^{15}\text{N}$ values with depth. As a result, photolysis leads to the snowpack emission of NO_x which may have a higher $\delta^{15}\text{N}$ value than that in skin layer nitrate. Furthermore, the skin layer does not experience a pure nitrate mass loss but also a gain in nitrate through atmospheric deposition. Deposition could result in a fractionation of the nitrogen isotopes in nitrate thus complicating the interpretation of observations at the air–snow interface.

10 During winter, nitrate photolysis cannot be invoked to explain the shift in $\delta^{15}\text{N}$ between the atmosphere and skin layer nitrate. However, the shift in $\delta^{15}\text{N}(\text{NO}_3^-)$ observed in winter could be linked to the existence of a fractionation of the nitrogen isotopes during deposition. Our data suggest that the $^{15}\text{N}/^{14}\text{N}$ fractionation constant associated with the deposition reaction $\text{HNO}_{3,(g)} \rightarrow \text{NO}_{3,(skin)}^-$ and denoted $^{15}\epsilon_{\text{dep}}$ must be positive and this sign may relate to the nature of the deposition of atmospheric nitrate to the snow. However, this discussion is beyond the scope of the present paper because the average $\delta^{15}\text{N}$ shift at the air–snow interface (24.7‰) is small when compared to the asymptotic $\delta^{15}\text{N}$ values measured at Dome C and Vostok (up to +300‰).

20 Conversely, $\Delta^{17}\text{O}$ values for atmospheric and skin layer nitrate are close but with a significant offset (with respect to the analytical uncertainty) on the order of 1–2‰ for most of the year with skin layer nitrate possessing slightly higher $\Delta^{17}\text{O}$ values than atmospheric nitrate (Fig. 10b). However, in early spring (end of September, beginning of October), the offset can exceed 5‰ and could be linked to reservoir effects during nitrate deposition. Indeed, the skin layer reservoir is on average 100 times larger than the atmospheric compartment when considering a constant boundary layer of 50 m and a constant skin layer snow density of 250 kg m^{-3} . The almost constant offset in $\Delta^{17}\text{O}$ throughout the year may therefore indicate an isotopic equilibrium at the DC air–snow interface but nevertheless with a small fractionation which must be taken into account

Air-snow transfer of nitrate in East Antarctica – Part 1

J. Erbland et al.

[Title Page](#)[Abstract](#)[Introduction](#)[Conclusions](#)[References](#)[Tables](#)[Figures](#)[⏪](#)[⏩](#)[◀](#)[▶](#)[Back](#)[Close](#)[Full Screen / Esc](#)[Printer-friendly Version](#)[Interactive Discussion](#)

in order to use $\Delta^{17}\text{O}$ in skin layer nitrate as a recorder of $\Delta^{17}\text{O}$ in atmospheric nitrate. This could be of particular interest at sites where atmospheric sampling is not feasible. Last, we acknowledge that skin layer nitrate is a more reliable recorder of the oxygen isotopic composition of atmospheric nitrate than is nitrate in the first 10 cm of snow (Frey et al., 2009) because $\Delta^{17}\text{O}$ is already affected by post-depositional processes at this depth (e.g. Panels 13 to 17 in Fig. 3).

The concentration maximum in atmospheric nitrate precedes that in the skin layer by 3–4 weeks (Fig. 9b). This temporal offset could be attributed to a faster flux of reactive nitrogen from the snow to the atmosphere under the effect of UV-photolysis when compared to a slower nitrate deposition flux over this period. To test this hypothesis, we have assumed a pure dry deposition of nitrate from the atmosphere to the snow with a constant deposition velocity of $v_{\text{dep, app}}$ (expressed in cm s^{-1}). We then calculate the cumulative nitrate mass deposited from the atmosphere to the snow starting from the end of the winter and compare this quantity to the nitrate mass in the skin layer over the same period of time. The temporal shift in nitrate concentration observed between the two compartments can be reproduced by using a $v_{\text{dep, app}}$ value of 0.15 cm s^{-1} (Fig. 12). This value is lower than the 0.8 cm s^{-1} value calculated for the dry deposition of HNO_3 in South Pole conditions (Huey et al., 2004). However, it should be borne in mind that our estimate represents an “apparent” deposition velocity for summer conditions at DC because a reemission flux of reactive nitrogen from the skin layer to the atmosphere also occur.

4.3 Interpretation of the asymptotic isotopic composition of nitrate on the Antarctic Plateau

4.3.1 $\delta^{15}\text{N}(\text{as.})$ sensitivity to snow accumulation rates

Snow accumulation rate is an important driver of $\delta^{15}\text{N}$ in snow nitrate as evidenced by the strong correlation between the asymptotic $\delta^{15}\text{N}$ values and the inverse of snow

Air-snow transfer of nitrate in East Antarctica – Part 1

J. Erbland et al.

Title Page

Abstract

Introduction

Conclusions

References

Tables

Figures

◀

▶

◀

▶

Back

Close

Full Screen / Esc

Printer-friendly Version

Interactive Discussion



Air-snow transfer of nitrate in East Antarctica – Part 1

J. Erbland et al.

Title Page

Abstract

Introduction

Conclusions

References

Tables

Figures

◀

▶

◀

▶

Back

Close

Full Screen / Esc

Printer-friendly Version

Interactive Discussion



accumulation rates: $\ln(\delta^{15}\text{N}(\text{as.}) + 1) = (5.76 \pm 0.47) \cdot (\text{kgm}^{-2} \text{a}^{-1} / A) + (0.01 \pm 0.02)$ ($1 - \sigma$ uncertainties calculated as in Taylor, 1997) (Fig. 6a). We note that this correlation has been previously emphasised in the pioneering work of Freyer et al. (1996) on the basis of the measurement of nitrogen isotopic ratios in nitrate archived in ice cores from Dome C, South Pole, Summit (Greenland) and D47, a location between D10 and DC. These archived values can then be considered to be asymptotic values as defined in this study, when assuming that nitrate and its isotopic composition are preserved in the firn and in the ice. The sensitivity of $\delta^{15}\text{N}(\text{as.})$ to $1/A$ reported in this study is close to the finding of Freyer et al. (1996), who reported a slope of 4.68. The detailed discussion of the small differences in slope is beyond the scope of this study.

Local variations in snow accumulation rate may contribute to explain the variations in $\delta^{15}\text{N}(\text{as.})$ observed at the same site. For instance, in Vostok, we report three snow pits which have comparable $^{15}\epsilon_{\text{app}}$ values (-63.2‰ , -59.7‰ and -62.2‰ for S4, V09-1 and V09-2, respectively, Table 1) but which have different $\delta^{15}\text{N}(\text{as.})$ values (256.6‰ , 380.4‰ and 307.3‰ , respectively). A closer look at these profiles (Panel 17 on Fig. 2) shows that the asymptotic $\delta^{15}\text{N}$ values are obtained following different trajectories with variations typically largest in the upper 10 cm. These contrasting variations in $\delta^{15}\text{N}$ with depth have also been observed by Frey et al. (2009) using of the DC04 and DC07-1 snow pits. The DC snow pit data reported in this study confirm this view. Frey et al. (2009) have attributed this feature to local surface heterogeneities linked to sastrugi formation and wind drift. We therefore propose that the high variability in $\delta^{15}\text{N}(\text{as.})$ that can be observed at one individual site such as Vostok is the result of variability in local snow accumulation rates at the spatial scale of a few meters. This could explain the higher uncertainty observed in this study when constraining the Antarctic Plateau pits with the relationship found between $\ln(\delta^{15}\text{N}(\text{as.}) + 1)$ and $1/A$: $\ln(\delta^{15}\text{N} + 1) = (4.22 \pm 1.43) \cdot (\text{kgm}^{-2} \text{a}^{-1} / A) + (0.08 \pm 0.06)$.

4.3.2 $\Delta^{17}\text{O}(\text{as.})$ potential to trace shifts in tropospheric oxidation

We have shown that the temporal variations in $\Delta^{17}\text{O}(\text{NO}_3^-)$ in the snow skin layer at DC are correlated with those in the atmosphere due to the local recycling of nitrate initiated by the UV-photolysis of snowpack nitrate in spring and summer; however, the two time series are slightly offset, most likely due to fractionation occurring upon deposition and reservoir effects. To investigate the transfer of the $\Delta^{17}\text{O}$ atmospheric signal below the photic zone, we compare the $\Delta^{17}\text{O}(\text{NO}_3^-)$ values in the two extreme compartments: the skin layer and the asymptotic nitrate (Fig. 13). The skin layer was not always sampled for the snow pits presented in this study; therefore, we use the samples representing the top 2 cm of snow which are equivalent as observed on Fig. 3. Figure 13b shows the comparison between the $\Delta^{17}\text{O}$ of nitrate in the top 2 cm of snow and the asymptotic $\Delta^{17}\text{O}$ values obtained for each snow pit.

In the coastal zone, we observe that $\Delta^{17}\text{O}(\text{NO}_3^-)$ is preserved in the snow as shown by the equivalent $\Delta^{17}\text{O}(\text{NO}_3^-)$ values in the top of the snowpack and below the active zone (Fig. 13b), consistent with $^{17}E_{\text{app}}$ values near zero ($(-0.2 \pm 1.5)\text{‰}$ on average). $\Delta^{17}\text{O}(\text{NO}_3^-)$ for the top 2 cm of snow at sites close to D10 show values as high as 38‰ (Figs. 3 and 13b). A greater preservation of nitrate stratospheric inputs, or possibly nitrate formed through reactions involving halogens (e.g. bromine), must be invoked to explain such high values (Savarino et al., 2007; Morin et al., 2009; Frey et al., 2009).

On the plateau, $\Delta^{17}\text{O}(\text{NO}_3^-)$ in the top 2 cm of snow is constant with an average $\Delta^{17}\text{O}$ value of 30‰, in accordance with previous spatial collections of the upper 10 cm of snow conducted by Frey et al. (2009) in the same area. In this zone, $\Delta^{17}\text{O}(\text{NO}_3^-)$ profiles show a significant decrease (between 5‰ and 10‰) with depth, which erases the extremes observed in the atmospheric signal (Frey et al., 2009). For instance, $\Delta^{17}\text{O}$ is reduced from 29 to 22‰ in the top 50 cm of Site 15 (Panel 15 on Fig. 3 and Fig. 13b). The atmospheric $\Delta^{17}\text{O}$ signal is therefore not entirely preserved during the transfer of nitrate from the surface to the snow below the photic zone (Fig. 13b). The observations

Air-snow transfer of nitrate in East Antarctica – Part 1

J. Erbland et al.

[Title Page](#)[Abstract](#)[Introduction](#)[Conclusions](#)[References](#)[Tables](#)[Figures](#)[◀](#)[▶](#)[◀](#)[▶](#)[Back](#)[Close](#)[Full Screen / Esc](#)[Printer-friendly Version](#)[Interactive Discussion](#)

for $\Delta^{17}\text{O}$ are consistent with those for $\delta^{18}\text{O}$ (Fig. 13c): asymptotic $\delta^{18}\text{O}$ values are strongly reduced when compared to the rather constant $\delta^{18}\text{O}$ values for nitrate in the top two cm of snow (around 40‰ on average). In addition, the positive $^{17}E_{\text{app}}$ and $^{18}\epsilon_{\text{app}}$ values observed on the plateau, $(+2.0 \pm 1.0)\text{‰}$ and $(+8.7 \pm 2.4)\text{‰}$ on average, reflect the observed reductions. We propose that the $\Delta^{17}\text{O}$ reduction in Antarctic Plateau sites is the result of cage recombination during nitrate photolysis (McCabe et al., 2005; Frey et al., 2009) which has been shown here to characterize this area. At this stage, we cannot rule out the possibility that another process is responsible for the depletion of the ^{18}O isotopes in the nitrate remaining in the snow.

5 Summary and conclusions

The physical release of nitrate and its UV-photolysis are associated with two distinct $^{15}\text{N}/^{14}\text{N}$ fractionation constants. While the two signatures of the loss processes are negative, $^{15}\epsilon_{\text{eva}}$ is closer to zero $(-8.5 \pm 2.5)\text{‰}$ than its modelled value of $^{15}\epsilon_{\text{pho}}$ $(< -48\text{‰})$, Frey et al., 2009). Based on these two distinct isotopic signatures and on the $^{15}\text{N}/^{14}\text{N}$ apparent fractionation constants ($^{15}\epsilon_{\text{app}}$) derived from nitrate mass fraction and $\delta^{15}\text{N}$ measurements in snow pits, it is possible to determine the loss process which dominates nitrate mass loss at a given site. Nitrogen isotopic data from East Antarctic Plateau sites presented in this study show that nitrate UV-photolysis is the dominant mass loss process in this area. In contrast, on the Antarctic coast, nitrate loss is less pronounced and could involved both photochemical and physical release processes. Apparent fractionation constants derived from the oxygen isotopic ratios measured in nitrate ($^{17}E_{\text{app}}$ and $^{18}\epsilon_{\text{app}}$) further support these conclusions with values non significantly different from zero and significantly positive at the coast and on the plateau, respectively. The latter reflects possible exchange of oxygen atoms between nitrate photo-products and H_2O in the snow grains lattice.

Air-snow transfer of nitrate in East Antarctica – Part 1

J. Erbland et al.

[Title Page](#)[Abstract](#)[Introduction](#)[Conclusions](#)[References](#)[Tables](#)[Figures](#)[◀](#)[▶](#)[◀](#)[▶](#)[Back](#)[Close](#)[Full Screen / Esc](#)[Printer-friendly Version](#)[Interactive Discussion](#)

Air-snow transfer of nitrate in East Antarctica – Part 1

J. Erbland et al.

Title Page

Abstract

Introduction

Conclusions

References

Tables

Figures

◀

▶

◀

▶

Back

Close

Full Screen / Esc

Printer-friendly Version

Interactive Discussion



On the plateau, nitrate UV-photolysis initiates a complex local recycling of nitrate. Annual nitrate collections in the atmosphere and skin layer (3–4 first mm of snow) at Dome C show an important consequence of this recycling: skin layer and atmospheric nitrates are in equilibrium in terms of oxygen isotopic ratios but with a non-zero fractionation constant due to unknown processes during deposition. $\delta^{15}\text{N}(\text{NO}_3^-)$ does not follow the same trend and a constant shift of more than 24‰ is observed and has tentatively been attributed to an isotopic fractionation upon deposition. The deposition of nitrate from the atmosphere to the skin layer also explains the temporal shift of 3–4 weeks between the atmospheric and snow nitrate concentration time series.

In this study, we have calculated asymptotic values from the nitrate isotopic profiles obtained for each snow pit. In present-day snow on the Antarctic Plateau, asymptotic $\delta^{15}\text{N}$ values ($\delta^{15}\text{N}(\text{as.})$) are the result of the highly negative $^{15}\text{N}/^{14}\text{N}$ fractionation constant (average $^{15}\varepsilon_{\text{app}}$ value of (-59 ± 10) ‰) set by nitrate UV-photolysis (and imposed by the spectral distribution of the actinic flux, modulated by the ozone column above the plateau, Frey et al., 2009) and by the nitrate mass fractions lost by photolysis which are linked to the photolytic rate constant (Eq. 1). This rate constant is modulated not only by the UV intensity received at the snowpack surface but also by the availability of nitrate for photolysis (Φ) and its residence time of snow layers in the photic zone. Following the approach of Freyer et al. (1996), we have shown that $\delta^{15}\text{N}(\text{as.})$ and $1/A$ are correlated confirming the strong control of the snow accumulation rate on nitrate exposure time in the photic zone. Other variables such as snow density may also impact the nitrate fractions lost via photolysis through the control on light penetration and residence time in the active zone. Second-order variables may also be the timing of the snow accumulation in the season as well as the wind redistribution of snow at the surface of snowpacks. We recall that the consistent shift (on the order of 25‰) observed between atmospheric and skin layer $\delta^{15}\text{N}(\text{NO}_3^-)$ time series at Dome C (Fig. 9c) are small when compared to the change of several hundreds of ‰ imposed by nitrate UV-photolysis so that this effect can be considered as of second-order in the asymptotic $\delta^{15}\text{N}$ values.

Air-snow transfer of nitrate in East Antarctica – Part 1

J. Erbland et al.

Title Page

Abstract

Introduction

Conclusions

References

Tables

Figures

◀

▶

◀

▶

Back

Close

Full Screen / Esc

Printer-friendly Version

Interactive Discussion



Our findings may have some implications for the interpretation of Greenland ice-core records. For instance, in an ice core retrieved from Summit, Greenland, Hastings et al. (2005) have ruled out nitrate post-depositional processing in the interpretation of their measured changes in $\delta^{15}\text{N}(\text{NO}_3^-)$ in between the present Holocene and the last glacial 36 kyr BP (+9.7 to +28.4‰ on average, respectively). At glacial times (20–35 kyr), snow accumulation rates and surface temperatures at Summit were around $80 \text{ kg m}^{-2} \text{ a}^{-1}$ and -46°C , while they are approximately $200\text{--}300 \text{ kg m}^{-2} \text{ a}^{-1}$ and -31°C for the present Holocene (last 2 kyr), respectively (Hastings et al., 2005; Kobashi et al., 2010). Glacial and present Holocene conditions at Summit therefore were equivalent to the present-day conditions found at sites 8–9 and 4–5, respectively (Table 1). Using the reduced $\delta^{15}\text{N}$ asymptotic data found for these East Antarctic sites, we calculate that this change in snow accumulation rates and surface temperatures would have lead to a positive shift of up to 70‰ in nitrate below the zone of active snow loss. Post-depositional nitrate mass loss could therefore well explain the +18.7‰ shift observed in Summit ice between the last glacial and the present Holocene. In the same study, Hastings et al. have also observed a strong correlation between nitrate $\delta^{15}\text{N}$ and snow accumulation rates in their Summit samples. Moreover, the identification of a present-day atmospheric nitrate source possessing the high $\delta^{15}\text{N}$ signature (+28.4‰) observed in glacial ice at Summit still remains elusive (Morin et al., 2009). Those observations support our assertion that the $\delta^{15}\text{N}$ data presented by Hastings et al. (2005) for the Summit ice core must be interpreted in light of the possible variations in the post-depositional processing of nitrate.

On the plateau, $\Delta^{17}\text{O}$ in skin layer nitrate is remarkably stable during summer when the samples were collected (around 30‰) and it may directly reflect the $\Delta^{17}\text{O}$ in the atmospheric nitrate at each site and possibly the local oxidative state of the atmosphere. However, this study has confirmed the conclusions of Frey et al. (2009) who have shown a reduction of $\Delta^{17}\text{O}(\text{NO}_3^-)$ at depth, possibly under cage recombination effects. This reduction of $\Delta^{17}\text{O}$, together with the important local recycling of nitrate at the air–snow interface on the plateau complicates the extraction from $\Delta^{17}\text{O}(\text{as.})$ of

information regarding the oxidative state of the atmosphere. Because temperature gradients and wind pumping exist in the top meters of plateau snowpacks, nitrate could still be mobilized but any net loss is expected to be small compared to the intense loss through UV-photolysis. Furthermore, nitrate in ice can be considered archived since it would diffuse from 3 cm to 14 cm over 100 kyr and at temperatures ranging from -50°C to -20°C (Thibert and Domine, 1998). Nitrate recored in ice cores could therefore represent a reliable image of nitrate which escaped the photic zone in past conditions. The interpretation of the nitrate isotopic records in ice cores would hence require a sound interpretation of the asymptotic nitrate isotopic composition archived in modern snow pits.

Given the complexity of the processing undergone by nitrate at the air–snow interface in East Antarctica, a numerical model including the isotopic composition of nitrate is required to deconvolute the integrated effects of recycling and cage recombination and to interpret the information retained in the archived nitrate. The companion paper (Erbland et al., 2012) presents an isotopic model relying on the conceptual model proposed by Davis et al. (2008) and Frey et al. (2009), which is tested by comparing its results with the atmospheric, skin layer and snow pit data obtained in the present study. This companion paper shows that there is potential in using $\Delta^{17}\text{O}$ in nitrate escaping the photic zone to derive information about local and summertime tropospheric oxidation. This model could then be used in past conditions to provide a framework for the interpretation of deep ice core records in terms of past shifts in the oxidative state of the atmosphere (undergoing).

Supplementary material related to this article is available online at:

**[http://www.atmos-chem-phys-discuss.net/12/28559/2012/
acpd-12-28559-2012-supplement.pdf](http://www.atmos-chem-phys-discuss.net/12/28559/2012/acpd-12-28559-2012-supplement.pdf).**

Air-snow transfer of nitrate in East Antarctica – Part 1

J. Erbland et al.

Title Page

Abstract

Introduction

Conclusions

References

Tables

Figures

◀

▶

◀

▶

Back

Close

Full Screen / Esc

Printer-friendly Version

Interactive Discussion



Acknowledgements. We thank A. Maggi, J.-Y. Thore (Université de Strasbourg, France) and K. Agabi (Université Nice Sophia Antipolis, France) as well as the winterover crews of the Concordia (Dome C) base for their help with the snow sampling in the field. The French Polar Institute (IPEV) is thanked for its logistical support in Antarctica. V. Lipenkov (AARI, St Petersburg, Russia) is thanked for having provided the V09-1 and V09-2 snow pits from Vostok. We thank G. Krinner for having downloaded the ERA-Interim temperature data, G. Picard for having processed them and G. Krinner and S. Parouty for providing the snow accumulation data. The Agence Nationale de la Recherche (ANR) is gratefully acknowledged for its financial support through the VANISH (Contract ANR-07-VULN-013) and OPALE (Contract ANR-09-BLAN-0226) projects. This study has also benefited partial funding from LICENCE (LEFE-CHAT), a scientific program of the Institut National des Sciences de l'Univers (INSU/CNRS), as well as from the IPCS program (CNRS) and from IPEV (Program NITEDC – 1011).



The publication of this article is financed by CNRS-INSU.

References

- Alexander, B., Savarino, J., Kreutz, K. J., and Thiemens, M. H.: Impact of preindustrial biomass-burning emissions on the oxidation pathways of tropospheric sulfur and nitrogen, *J. Geophys. Res.*, 109, D08303, doi:10.1029/2003JD004218, 2004. 28562
- Alexander, B., Hastings, M. G., Allman, D. J., Dachs, J., Thornton, J. A., and Kunasek, S. A.: Quantifying atmospheric nitrate formation pathways based on a global model of the oxygen isotopic composition ($\Delta^{17}\text{O}$) of atmospheric nitrate, *Atmos. Chem. Phys.*, 9, 5043–5056, doi:10.5194/acp-9-5043-2009, 2009. 28562

Air-snow transfer of nitrate in East Antarctica – Part 1

J. Erbland et al.

Title Page

Abstract

Introduction

Conclusions

References

Tables

Figures

◀

▶

◀

▶

Back

Close

Full Screen / Esc

Printer-friendly Version

Interactive Discussion



**Air-snow transfer of
nitrate in East
Antarctica – Part 1**

J. Erbland et al.

Title Page

Abstract

Introduction

Conclusions

References

Tables

Figures

◀

▶

◀

▶

Back

Close

Full Screen / Esc

Printer-friendly Version

Interactive Discussion



- Blunier, T., Floch, G. L., Jacobi, H.-W., and Quansah, E.: Isotopic view on nitrate loss in Antarctic surface snow, *Geophys. Res. Lett.*, 32, L13501, doi:10.1029/2005GL023011, 2005. 28561, 28562, 28563, 28567, 28568, 28569, 28570, 28593, 28600, 28601, 28602
- 5 Casciotti, K. L., Sigman, D. M., Hastings, M. G., Böhlke, J. K., and Hilkert, A.: Measurement of the oxygen isotopic composition of nitrate in seawater and freshwater using the denitrifier method, *Anal. Chem.*, 74, 4905–4912, doi:10.1021/ac020113w, 2002. 28567
- Chu, L. and Anastasio, C.: Quantum yields of hydroxyl radical and nitrogen dioxide from the photolysis of nitrate on ice, *J. Phys. Chem.*, 107, 9594–9602, 2003. 28563
- 10 Criss, R. E.: *Principles of Stable Isotope Distribution*, Oxford University Press, New York, 1999. 28563
- Davis, D. D., Seelig, J., Huey, G., Davis, D. D., Seelig, J., Huey, G., Crawford, J., Chen, G., Wang, Y., Buhr, M., Helmig, D., Neff, W., Blake, D., Arimoto, R., and Eisele F.: A reassessment of Antarctic Plateau reactive nitrogen based on ANTCI 2003 airborne and ground based measurements, *Atmos. Environ.*, 42, 2831–2848, doi:10.1016/j.atmosenv.2007.07.039, 2008. 15 28563, 28578, 28586
- Dee, D. P., Uppala, S. M., Simmons, A. J., Berrisford, P., Poli, P., Kobayashi, S., Andrae, U., Balmaseda, M. A., Balsamo, G., Bauer, P., Bechtold, P., Beljaars, A. C. M., van de Berg, L., Bidlot, J., Bormann, N., Delsol, C., Dragani, R., Fuentes, M., Geer, A. J., Haimberger, L., Healy, S. B., Hersbach, H., Hólm, E. V., Isaksen, I., Kållberg, P., Köhler, M., Matricardi, M., McNally, A. P., Monge-Sanz, B. M., Morcrette, J.-J., Park, B.-K., Peubey, C., de Rosnay, P., 20 Tavolato, C., Thépaut, J.-N., and Vitart, F.: The ERA-Interim reanalysis: configuration and performance of the data assimilation system, *Q. J. Roy. Meteor. Soc.*, 137, 553–597, doi:10.1002/qj.828, 2011. 28569, 28593
- Dibb, J. E., Talbot, R. W., Munger, J. W., Jacob, D. J., and Fan, S. M.: Air-snow exchange of HNO_3 and NO_y at Summit, Greenland, *J. Geophys. Res.*, 103, 3475–3486, doi:10.1029/97JD03132, 1998. 28561
- 25 Domine, F., Albert, M., Huthwelker, T., Jacobi, H.-W., Kokhanovsky, A. A., Lehning, M., Picard, G., and Simpson, W. R.: Snow physics as relevant to snow photochemistry, *Atmos. Chem. Phys.*, 8, 171–208, doi:10.5194/acp-8-171-2008, 2008. 28568
- 30 Ekaykin, A. A., Lipenkov, V. Y., Barkov, N., Petit, J.-R., and Masson-Delmotte, V.: Spatial and temporal variability in isotope composition of recent snow in the vicinity of Vostok station, Antarctica: implications for ice-core record interpretation, *Ann. Glaciol.*, 35, 181–186, doi:10.3189/172756402781816726, 2002. 28569

Air-snow transfer of nitrate in East Antarctica – Part 1

J. Erbland et al.

[Title Page](#)[Abstract](#)[Introduction](#)[Conclusions](#)[References](#)[Tables](#)[Figures](#)[◀](#)[▶](#)[◀](#)[▶](#)[Back](#)[Close](#)[Full Screen / Esc](#)[Printer-friendly Version](#)[Interactive Discussion](#)

- EPICA community members: Eight glacial cycles from an Antarctic ice core, *Nature*, 429, 623–628, doi:10.1038/nature02599, 2004. 28569
- Erbland, J., Savarino, J., Morin, S., France, J. L., and Frey, M. M.: Air-snow transfer of nitrate on the East Antarctic Plateau – Part 2: An isotopic model for the interpretation of deep ice-core records, *Atmos. Chem. Phys.*, in preparation, 2012. 28564, 28586
- France, J. L., King, M. D., Frey, M. M., Erbland, J., Picard, G., Preunkert, S., MacArthur, A., and Savarino, J.: Snow optical properties at Dome C (Concordia), Antarctica; implications for snow emissions and snow chemistry of reactive nitrogen, *Atmos. Chem. Phys.*, 11, 9787–9801, doi:10.5194/acp-11-9787-2011, 2011. 28568
- Frey, M. M., Savarino, J., Morin, S., Erbland, J., and Martins, J. M. F.: Photolysis imprint in the nitrate stable isotope signal in snow and atmosphere of East Antarctica and implications for reactive nitrogen cycling, *Atmos. Chem. Phys.*, 9, 8681–8696, doi:10.5194/acp-9-8681-2009, 2009. 28560, 28561, 28562, 28563, 28564, 28565, 28566, 28567, 28569, 28570, 28572, 28573, 28574, 28576, 28578, 28580, 28581, 28582, 28583, 28584, 28585, 28586, 28593, 28594, 28600, 28601, 28602, 28604, 28605
- Freyer, H. D., Kobel, K., Delmas, R. J., Kley, D., and Legrand, M. R.: First results of $^{15}\text{N}/^{14}\text{N}$ ratios in nitrate from alpine and polar ice cores, *Tellus B*, 48, 93–105, 1996. 28561, 28581, 28584, 28601
- Gallet, J.-C., Domine, F., Arnaud, L., Picard, G., and Savarino, J.: Vertical profile of the specific surface area and density of the snow at Dome C and on a transect to Dumont D'Urville, Antarctica – albedo calculations and comparison to remote sensing products, *The Cryosphere*, 5, 631–649, doi:10.5194/tc-5-631-2011, 2011. 28577
- Grannas, A. M., Jones, A. E., Dibb, J., Ammann, M., Anastasio, C., Beine, H. J., Bergin, M., Bottenheim, J., Boxe, C. S., Carver, G., Chen, G., Crawford, J. H., Dominé, F., Frey, M. M., Guzmán, M. I., Heard, D. E., Helmig, D., Hoffmann, M. R., Honrath, R. E., Huey, L. G., Hutterli, M., Jacobi, H. W., Klán, P., Lefer, B., McConnell, J., Plane, J., Sander, R., Savarino, J., Shepson, P. B., Simpson, W. R., Sodeau, J. R., von Glasow, R., Weller, R., Wolff, E. W., and Zhu, T.: An overview of snow photochemistry: evidence, mechanisms and impacts, *Atmos. Chem. Phys.*, 7, 4329–4373, doi:10.5194/acp-7-4329-2007, 2007. 28561
- Hastings, M. G., Steig, E. J., and Sigman, D. M.: Glacial/interglacial changes in the isotopes of nitrate from the Greenland Ice Sheet Project 2 (GISP2) ice core, *Global Biogeochem. Cy.*, 19, GB4024, doi:10.1029/2005GB002502, 2005. 28585

Air-snow transfer of nitrate in East Antarctica – Part 1

J. Erbland et al.

Title Page

Abstract

Introduction

Conclusions

References

Tables

Figures

◀

▶

◀

▶

Back

Close

Full Screen / Esc

Printer-friendly Version

Interactive Discussion



Huey, L. G., Tanner, D. J., Slusher, D. L., Dibb, J. E., Arimoto, R., Chen, G., Davis, D., Buhr, M. P., Nowak, J. B., Mauldin III, R. L., Eisele, F. L., and Kosciuch, E.: CIMS measurements of HNO_3 and SO_2 at the South Pole during ICAT 2000, *Atmos. Environ.*, 38, 5411–5421, doi:10.1016/j.atmosenv.2004.04.037, 2004. 28578, 28580

5 Kaiser, J., Hastings, M. G., Houlton, B. Z., Röckmann, T., and Sigman, D. M.: Triple oxygen isotope analysis of nitrate using the denitrifier method and thermal decomposition of N_2O , *Anal. Chem.*, 79, 599–607, doi:10.1021/ac061022s, 2007. 28567

Kobashi, T., Kawamura, K., Severinghaus, J. P., Barnola, J.-M., Nakaegawa, T., Vinther, B. M., Johnsen, S. J., and Box, J. E.: High variability of Greenland surface temperature over the
10 past 4000 years estimated from trapped air in an ice core, *Geophys. Res. Lett.*, 38, L21501, doi:10.1029/2011GL049444, 2010. 28585

Krinner, G., Magand, O., Simmonds, I., Genthon, C., and Dufresne, J.: Simulated Antarctic precipitation and surface mass balance at the end of the twentieth and twenty-first centuries, *Clim. Dynam.*, 28, 215–230, doi:10.1007/s00382-006-0177-x, 2007. 28569

15 Kunasek, S. A., Alexander, B., Steig, E. J., Hastings, M. G., Gleason, D. J., and Jarvis, J. C.: Measurements and modeling of $\Delta^{17}\text{O}$ of nitrate in snowpits from Summit, Greenland, *J. Geophys. Res.*, 113, D24302, doi:10.1029/2008JD010103, 2008. 28562

Mayewski, P. A. and Legrand, M. R.: Recent increase in nitrate concentration of Antarctic snow, *Nature*, 346, 258–260, 1990. 28561

20 McCabe, J. R., Boxe, C. S., Colussi, A. J., Hoffman, M. R., and Thiemens, M. H.: Oxygen isotopic fractionation in the photochemistry of nitrate in water and ice, *J. Geophys. Res.*, 110, D15310, doi:10.1029/2004JD005484, 2005. 28562, 28575, 28577, 28583

McCabe, J. R., Savarino, J., Alexander, B., Gong, S., and Thiemens, M. H.: Isotopic constraints on non-photochemical sulfate production in the Arctic winter, *Geophys. Res. Lett.*,
25 33, L05810, doi:10.1029/2005GL025164, 2006. 28572

McCabe, J. R., Thiemens, M. H., and Savarino, J.: A record of ozone variability in South Pole Antarctic snow: the role of nitrate oxygen isotopes, *J. Geophys. Res.*, 112, D12303, doi:10.1029/2006JD007822, 2007. 28562

Michalski, G., Scott, Z., Kabling, M., and Thiemens, M. H.: First measurements and modeling
30 of $\Delta^{17}\text{O}$ in atmospheric nitrate, *Geophys. Res. Lett.*, 30, 1870, doi:10.1029/2003GL017015, 2003. 28562

Miller, C. E. and Yung, Y. L.: Photo-induced isotopic fractionation, *J. Geophys. Res.*, 105, 29039–29051, 2000. 28563

Air-snow transfer of nitrate in East Antarctica – Part 1

J. Erbland et al.

[Title Page](#)[Abstract](#)[Introduction](#)[Conclusions](#)[References](#)[Tables](#)[Figures](#)[◀](#)[▶](#)[◀](#)[▶](#)[Back](#)[Close](#)[Full Screen / Esc](#)[Printer-friendly Version](#)[Interactive Discussion](#)

Morin, S., Savarino, J., Frey, M. M., Yan, N., Bekki, S., and Bottenheim, J. M.: Tracing the origin and fate of NO_x in the Arctic atmosphere using stable isotopes in nitrate, *Science*, 322, doi:10.1126/science.1161910, 2008. 28562

Morin, S., Savarino, J., Frey, M. M., Domine, F., Jacobi, H. W., Kaleschke, L., and Martins, J. M. F.: Comprehensive isotopic composition of atmospheric nitrate in the Atlantic Ocean boundary layer from 65°S to 79°N , *J. Geophys. Res.*, 114, D05303, doi:10.1029/2008JD010696, 2009. 28562, 28565, 28567, 28578, 28582, 28585

Morin, S., Sander, R., and Savarino, J.: Simulation of the diurnal variations of the oxygen isotope anomaly ($\Delta^{17}\text{O}$) of reactive atmospheric species, *Atmos. Chem. Phys.*, 11, 3653–3671, doi:10.5194/acp-11-3653-2011, 2011. 28562

Neubauer, J. and Heumann, K. G.: Determination of nitrate at the ng/g level in Antarctic snow samples with ion chromatography and isotope-dilution mass-spectrometry, *Fresenius Z. Anal. Chem.*, 331, 170–173, 1988. 28561

Pinzer, B. R., Schneebeli, M., and Kaempfer, T. U.: Vapor flux and recrystallization during dry snow metamorphism under a steady temperature gradient as observed by time-lapse microtomography, *The Cryosphere*, 6, 1141–1155, doi:10.5194/tc-6-1141-2012, 2012. 28577

Röthlisberger, R., Hutterli, M. A., Sommer, S., Wolff, E. W., and Mulvaney, R.: Factors controlling nitrate in ice-cores: evidence from the Dome C deep ice core, *J. Geophys. Res.*, 105, 20565–20572, 2000. 28561, 28569

Röthlisberger, R., Hutterli, M. A., Wolff, E. W., Mulvaney, R., Fischer, H., Bigler, M., Goto-Azuma, K., Hansson, M. E., Ruth, U., Siggaard-Andersen, M.-L., and Steffensen J. P.: Nitrate in Greenland and Antarctic ice cores: a detailed description of post-depositional processes, *Ann. Glaciol.*, 35, 209–216, 2002. 28561

Savarino, J., Kaiser, J., Morin, S., Sigman, D. M., and Thiemens, M. H.: Nitrogen and oxygen isotopic constraints on the origin of atmospheric nitrate in coastal Antarctica, *Atmos. Chem. Phys.*, 7, 1925–1945, doi:10.5194/acp-7-1925-2007, 2007. 28578, 28582

Sigman, D. M., Casciotti, K. L., Andreani, M., Barford, C., Galanter, M., and Böhlke, J. K.: A bacterial method for the nitrogen isotopic analysis of nitrate in marine and fresh waters, *Anal. Chem.*, 73, 4145–4153, 2001. 28567

Silva, S. R., Kendall, C., Wilkinson, D. H., Ziegler, A. C., Chang, C. C. Y., and Avanzino, R. J.: A new method for collection of nitrate from fresh water and analysis of the nitrogen and oxygen isotope ratios, *J. Hydrol.*, 228, 22–36, 2000. 28566

Simpson, W. R., King, M. D., Beine, H. J., Honrath, R. E., and Zhou, X.: Radiation-transfer modeling of snow pack photochemical processes during ALERT2000, *Atmos. Environ.*, 36, 2663–2670, 2002. 28568

Taylor, J. R.: *An Introduction to Error Analysis: the Study of Uncertainties in Physical Measurements*, 2nd edn., University Science Books, Sausalito, CA, 1997. 28581, 28593

Thibert, E. and Domine, F.: Thermodynamics and kinetics of the solid solution of HNO₃ in ice, *J. Phys. Chem. B*, 102, 4432–4439, 1998. 28586

Wolff, E.: Nitrate in polar ice, in: *Ice Core Studies of Global Biogeochemical Cycles*, Springer, New York, 195–224, 1995. 28561

Wolff, E. W., Jones, A. E., Bauguitte, S. J.-B., and Salmon, R. A.: The interpretation of spikes and trends in concentration of nitrate in polar ice cores, based on evidence from snow and atmospheric measurements, *Atmos. Chem. Phys.*, 8, 5627–5634, doi:10.5194/acp-8-5627-2008, 2008. 28572

Air-snow transfer of nitrate in East Antarctica – Part 1J. Erbland et al.

[Title Page](#)[Abstract](#)[Introduction](#)[Conclusions](#)[References](#)[Tables](#)[Figures](#)[⏪](#)[⏩](#)[◀](#)[▶](#)[Back](#)[Close](#)[Full Screen / Esc](#)[Printer-friendly Version](#)[Interactive Discussion](#)

Air-snow transfer of nitrate in East Antarctica – Part 1

J. Erbland et al.

Table 2. Nitrate evaporation experiments: isotopic fractionation constants calculated for each of the three evaporation experiments conducted at -10°C , -20°C and -30°C ($1\text{-}\sigma$ uncertainties calculated as in Frey et al., 2009).

Temp./ $^{\circ}\text{C}$	Duration/days	NO_3^- fraction lost/%	Snow fraction lost/%	$^{15}\epsilon_{\text{eva}} \pm 1\sigma/\text{‰}$
-10	10	40	72	-8.5 ± 2.5
-20	14	11	7	0.6 ± 1.8
-30	14	10	1	1.8 ± 3.0

Title Page

Abstract

Introduction

Conclusions

References

Tables

Figures

◀

▶

◀

▶

Back

Close

Full Screen / Esc

Printer-friendly Version

Interactive Discussion



Air-snow transfer of nitrate in East Antarctica – Part 1

J. Erbland et al.

Table 3. Apparent fractionation constants ${}^n\epsilon$ ($n = 15, 17, 18$ for $\delta^{15}\text{N}$, $\Delta^{17}\text{O}$ and $\delta^{18}\text{O}$, respectively) in East Antarctica: average, standard deviation, minimum and maximum values. For the plateau, we have also used all previously published data (see in Table 1).

	${}^{15}\epsilon_{\text{app}}/\text{‰}$	${}^{18}\epsilon_{\text{app}}/\text{‰}$	${}^{17}E_{\text{app}}/\text{‰}$
Plateau ($T_{\text{a}} \leq -45\text{ °C}$)			
ave.	-59.2	+8.7	+2.0
$\pm 1\text{-}\sigma$	+10.4	+2.4	+1.0
min.	-74.3	+3.9	+0.2
max.	-40.0	+12.3	+4.4
Coast ($T_{\text{a}} > -35\text{ °C}$)			
ave.	-16.1	+3.1	-0.2
$\pm 1\text{-}\sigma$	+13.5	+5.8	+1.5
min.	-34.2	-3.9	-2.0
max.	+0.3	+8.4	+2.0

[Title Page](#)
[Abstract](#)
[Introduction](#)
[Conclusions](#)
[References](#)
[Tables](#)
[Figures](#)
[Back](#)
[Close](#)
[Full Screen / Esc](#)
[Printer-friendly Version](#)
[Interactive Discussion](#)

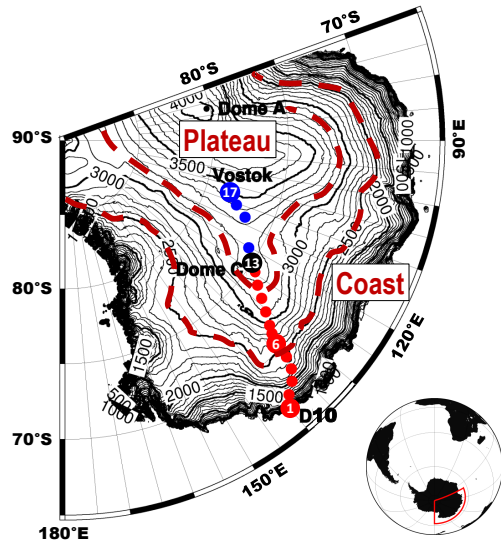



Fig. 1. Snow pit collections in 17 locations in East Antarctica. Spacing of the contour lines is 100 m. The red and blue symbols indicate the locations visited during the austral summers 2007–2008 and 2009–2010, respectively. The Dome C and Vostok sites were sampled two and three times, respectively. The red dashed lines represent the boundaries of the “coast” and “plateau” zones as defined in Sect. 2.4.

Air-snow transfer of nitrate in East Antarctica – Part 1

J. Erbland et al.

Title Page

Abstract

Introduction

Conclusions

References

Tables

Figures

◀

▶

◀

▶

Back

Close

Full Screen / Esc

Printer-friendly Version

Interactive Discussion



Air-snow transfer of nitrate in East Antarctica – Part 1

J. Erbland et al.

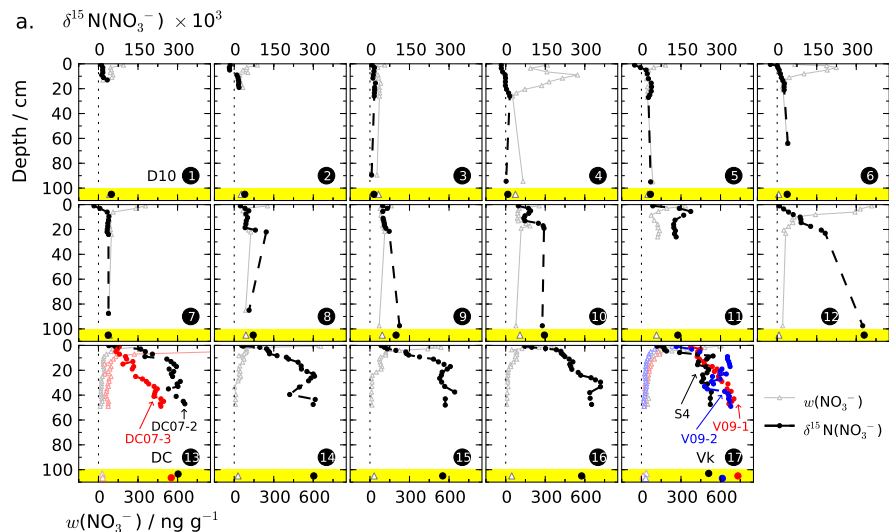


Fig. 2. Nitrate mass fraction and $\delta^{15}\text{N}$ profiles in the upper snowpack in East Antarctica. The numbers refer to the individual locations identified in Fig. 1 and Table 1. For the Dome C and Vostok sites, the colors refer to the different snow pits sampled in those locations: DC07-2 in black and DC07-3 in red; S4 in black, V09-1 in red and V09-2 in blue, respectively. The triangles and circles in the yellow shaded area below one meter in each panel represent the asymptotic nitrate mass fraction ($w(\text{as.})$) and $\delta^{15}\text{N}$ ($\delta^{15}\text{N}(\text{as.})$) calculated for each pit.

Title Page

Abstract

Introduction

Conclusions

References

Tables

Figures

◀

▶

◀

▶

Back

Close

Full Screen / Esc

Printer-friendly Version

Interactive Discussion



Air-snow transfer of nitrate in East Antarctica – Part 1

J. Erbland et al.

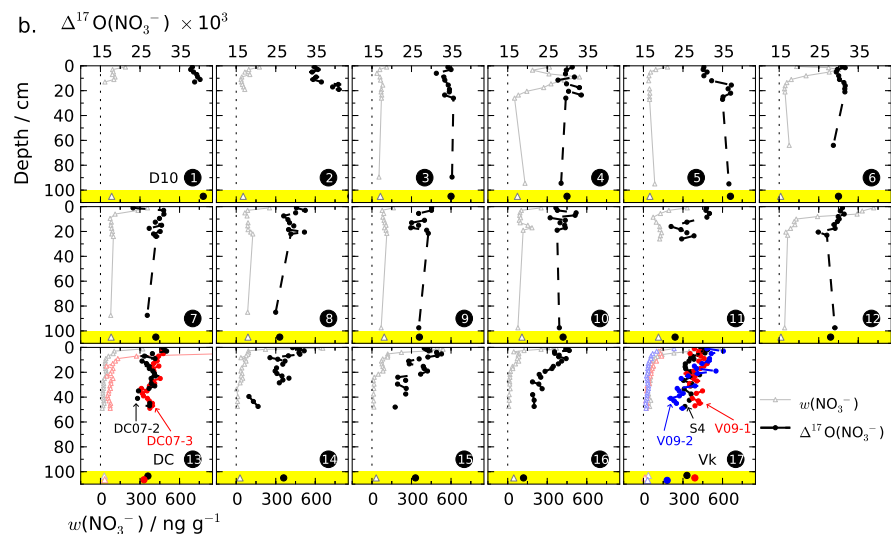


Fig. 3. Nitrate mass fraction and $\Delta^{17}\text{O}$ profiles in the upper snowpack in East Antarctica. The numbers refer to the individual locations identified in Fig. 1 and Table 1. For the Dome C and Vostok sites, the colors refer to the different snow pits sampled in those locations: DC07-2 in black and DC07-3 in red; S4 in black, V09-1 in red and V09-2 in blue, respectively. The triangles and circles in the yellow shaded area below one meter in each panel represent the asymptotic nitrate mass fraction ($w(\text{as.})$) and $\Delta^{17}\text{O}$ ($\Delta^{17}\text{O}(\text{as.})$) calculated for each pit.

Title Page

Abstract

Introduction

Conclusions

References

Tables

Figures

◀

▶

◀

▶

Back

Close

Full Screen / Esc

Printer-friendly Version

Interactive Discussion



Air-snow transfer of nitrate in East Antarctica – Part 1

J. Erbland et al.

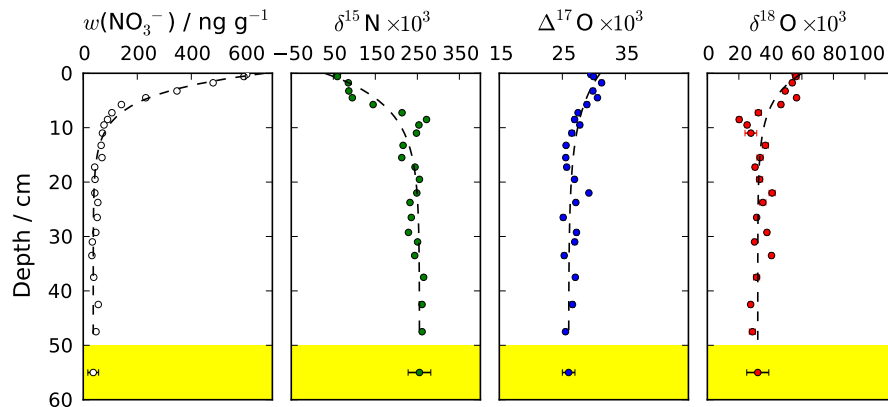


Fig. 4. Detailed view of nitrate mass fraction and isotopic composition profiles for snow pit S4 (Panel 17 on Figs. 2 and 3). The black dashed lines represent the fit to the data used to derive the asymptotic values as expressed in Eq. (2).

[Title Page](#)[Abstract](#)[Introduction](#)[Conclusions](#)[References](#)[Tables](#)[Figures](#)[◀](#)[▶](#)[◀](#)[▶](#)[Back](#)[Close](#)[Full Screen / Esc](#)[Printer-friendly Version](#)[Interactive Discussion](#)

Air-snow transfer of nitrate in East Antarctica – Part 1

J. Erbland et al.

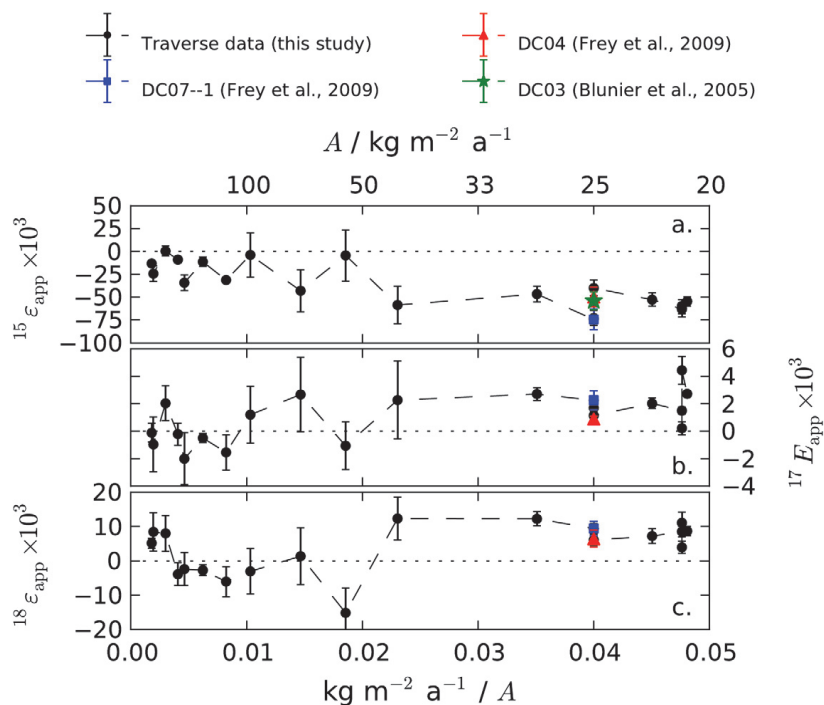


Fig. 5. Reduced data for the snow pits collected in East Antarctica. **(a–c)** $^{15}\text{N}/^{14}\text{N}$, ^{17}O –excess and $^{18}\text{O}/^{16}\text{O}$ apparent fractionation constants ($^{15}\epsilon_{\text{app}}$, $^{17}E_{\text{app}}$ and $^{18}\epsilon_{\text{app}}$, respectively). Data for previously published pits are marked by a blue square (DC07-1, Frey et al., 2009), a red triangle (DC04, Frey et al., 2009) and a green star (Blunier et al., 2005).

Title Page

Abstract

Introduction

Conclusions

References

Tables

Figures

◀

▶

◀

▶

Back

Close

Full Screen / Esc

Printer-friendly Version

Interactive Discussion



Air-snow transfer of nitrate in East Antarctica – Part 1

J. Erbland et al.

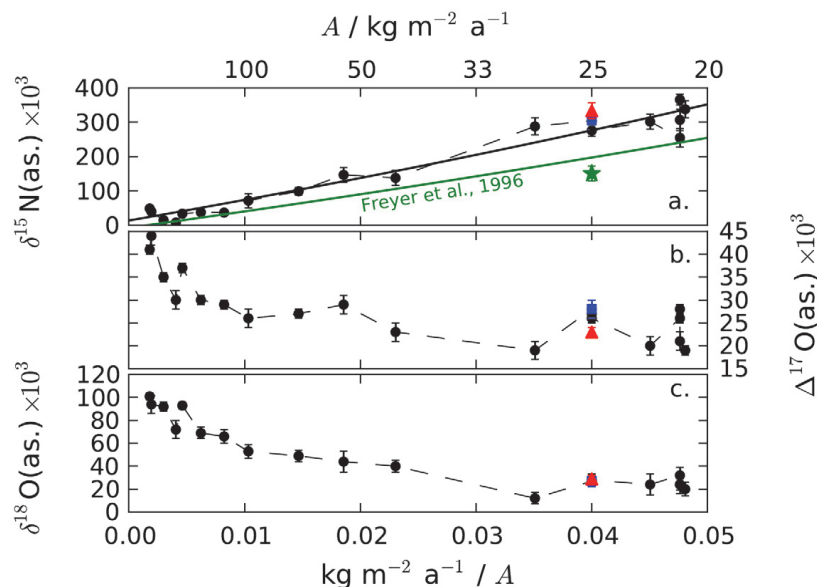


Fig. 6. (Continues Fig. 5) Reduced data for the snow pits collected in East Antarctica. **(a–c)** Asymptotic $\delta^{15}\text{N}$, $\Delta^{17}\text{O}$ and $\delta^{18}\text{O}$ values. Data for previously published pits are marked by a blue square (DC07-1, Frey et al., 2009), a red triangle (DC04, Frey et al., 2009) and a green star (Blunier et al., 2005). The solid lines in **(a)** are fits to this study's (black) and Freyer et al. (1996)'s (green) data following the approach of the latter authors.

Title Page

Abstract

Introduction

Conclusions

References

Tables

Figures

◀

▶

◀

▶

Back

Close

Full Screen / Esc

Printer-friendly Version

Interactive Discussion



Air-snow transfer of nitrate in East Antarctica – Part 1

J. Erbland et al.

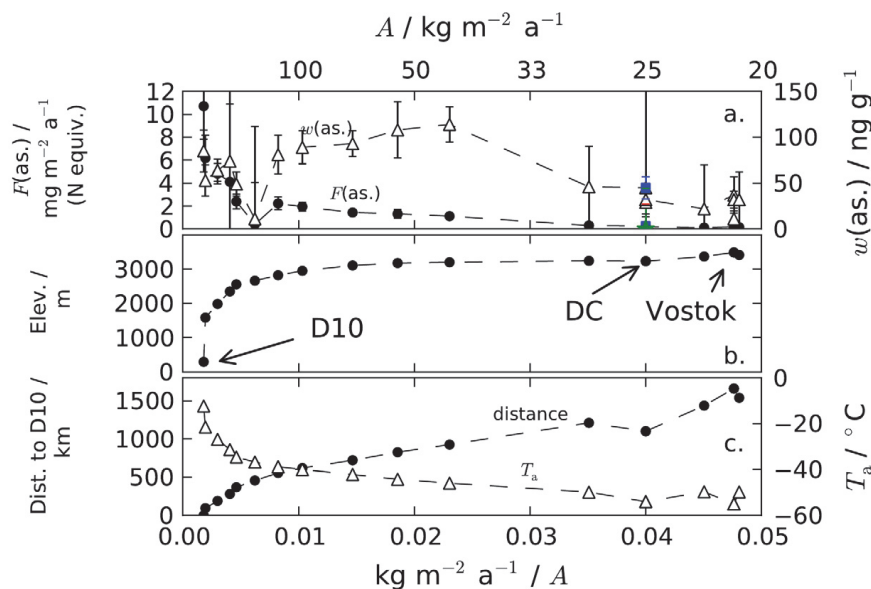


Fig. 7. (Continues Figs. 5 and 6) Reduced data for the snow pits collected in East Antarctica. **(a)** Asymptotic nitrate flux $F(\text{as.})$ and mass fractions $w(\text{as.})$, **(b)** site's elevation and **(c)** site's distance to D10 and mean annual temperature T_a . Data for previously published pits are marked by a blue square (DC07-1, Frey et al., 2009), a red triangle (DC04, Frey et al., 2009) and a green star (Blunier et al., 2005).

Title Page

Abstract

Introduction

Conclusions

References

Tables

Figures

◀

▶

◀

▶

Back

Close

Full Screen / Esc

Printer-friendly Version

Interactive Discussion



Air-snow transfer of nitrate in East Antarctica – Part 1

J. Erbland et al.

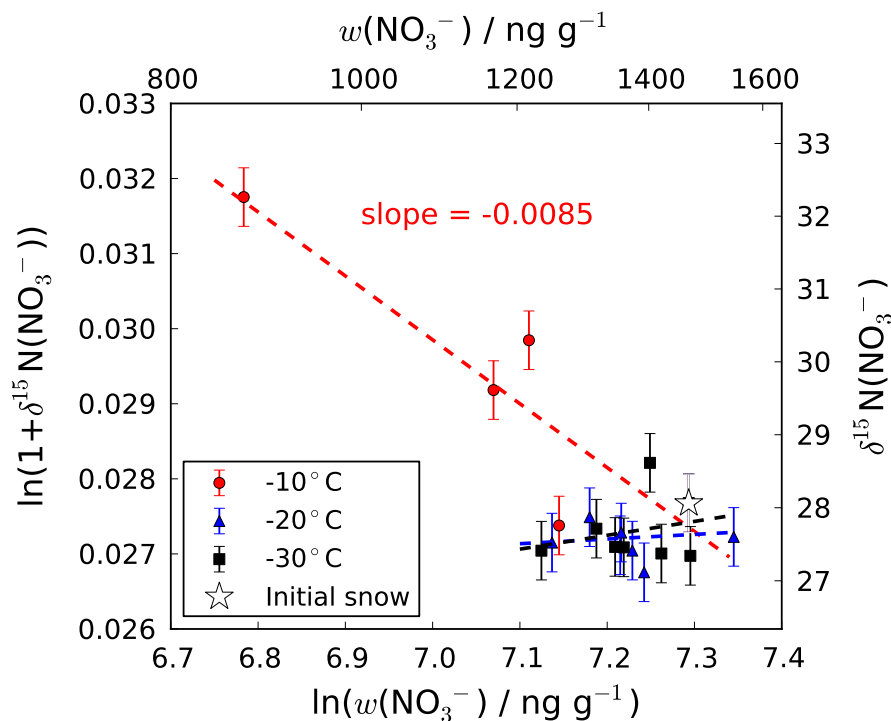


Fig. 8. Nitrate evaporation experiments: $1 + \delta^{15}\text{N}(\text{NO}_3^-)$ and $w(\text{NO}_3^-)$ are plotted in a logarithmic scale. The red line is a linear fit to the data obtained for the experiment conducted at -10°C where a Rayleigh-type single loss process is assumed.

Title Page

Abstract

Introduction

Conclusions

References

Tables

Figures

◀

▶

◀

▶

Back

Close

Full Screen / Esc

Printer-friendly Version

Interactive Discussion



Air-snow transfer of nitrate in East Antarctica – Part 1

J. Erbland et al.

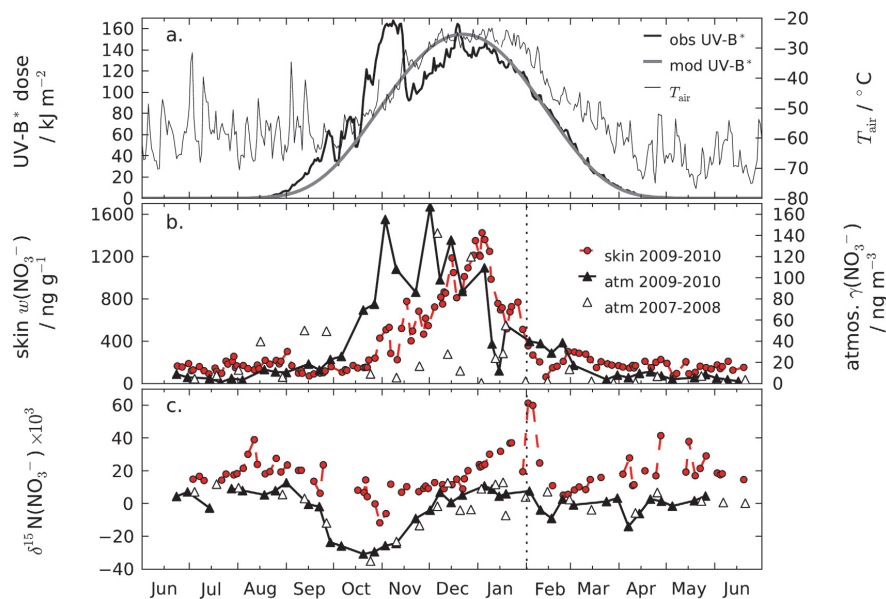


Fig. 9. DC atmospheric and skin layer NO_3^- in 2007–2008 (Frey et al., 2009) and 2009–2010 and skin layer nitrate in 2009–2010: **(a)** DC daily air temperature (thin line) and modelled UV-B* (280–320 nm) for observed and a constant (290 DU) O_3 column density (black and grey lines) and a snow albedo of 0.9, **(b)** NO_3^- concentrations, **(c)** $\delta^{15}\text{N}(\text{NO}_3^-)$ in atmospheric nitrate in 2007–2008 and 2009–2010 (open and closed triangles, respectively) and in skin layer nitrate in 2009–2010 (red circles). The vertical dashed line represents the date when the data were assembled to form the composite year 2009–2010.

Title Page

Abstract

Introduction

Conclusions

References

Tables

Figures

◀

▶

◀

▶

Back

Close

Full Screen / Esc

Printer-friendly Version

Interactive Discussion



Air-snow transfer of nitrate in East Antarctica – Part 1

J. Erbland et al.

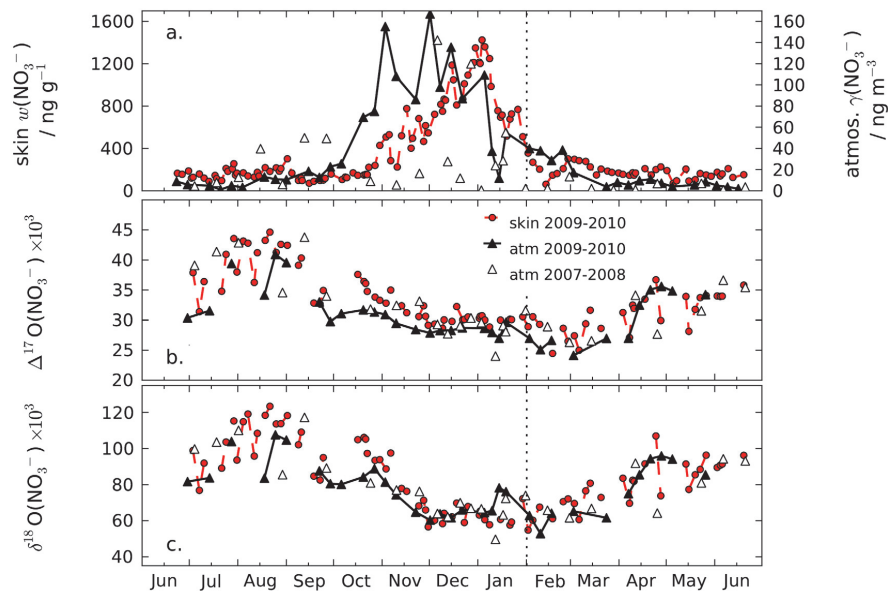


Fig. 10. (Continues Fig. 9 with the top panel being repeated for clarity) DC atmospheric and skin layer NO_3^- in 2007–2008 (Frey et al., 2009) and 2009–2010 and skin layer nitrate in 2009–2010: **(a)** NO_3^- concentrations, **(b)** $\Delta^{17}\text{O}(\text{NO}_3^-)$ and **(c)** $\delta^{18}\text{O}(\text{NO}_3^-)$ in atmospheric nitrate in 2007–2008 and 2009–2010 (open and closed triangles, respectively) and in skin layer nitrate in 2009–2010 (red circles). The vertical dashed line represents the date when the data were assembled to form the composite year 2009–2010.

Title Page

Abstract

Introduction

Conclusions

References

Tables

Figures

◀

▶

◀

▶

Back

Close

Full Screen / Esc

Printer-friendly Version

Interactive Discussion



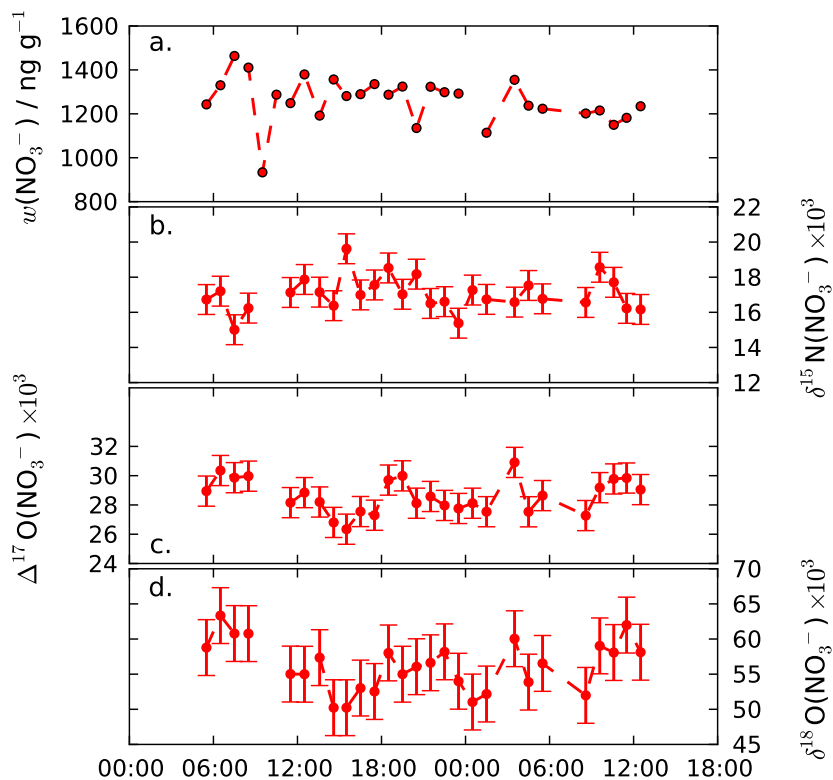


Fig. 11. Hourly variations of skin layer nitrate at DC on 28 and 29 December 2009: **(a)** NO_3^- mass fractions, **(b)** $\delta^{15}\text{N}(\text{NO}_3^-)$, **(c)** $\Delta^{17}\text{O}(\text{NO}_3^-)$ and **(d)** $\delta^{18}\text{O}(\text{NO}_3^-)$. Note the narrow ranges in the y-axes when compared to Figs. 9 and 10.

Air-snow transfer of nitrate in East Antarctica – Part 1

J. Erbland et al.

Title Page

Abstract

Introduction

Conclusions

References

Tables

Figures

◀

▶

◀

▶

Back

Close

Full Screen / Esc

Printer-friendly Version

Interactive Discussion



Air-snow transfer of nitrate in East Antarctica – Part 1

J. Erbland et al.

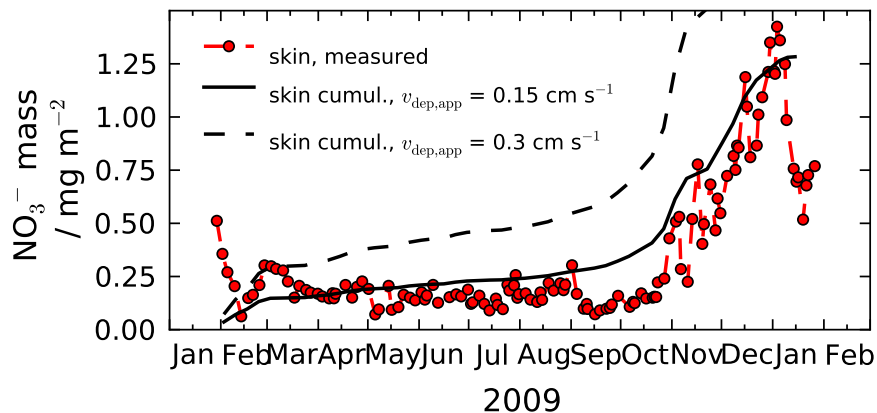


Fig. 12. Cumulative dry deposition from the atmosphere to the skin layer for two different vertical apparent deposition velocities.

[Title Page](#)[Abstract](#)[Introduction](#)[Conclusions](#)[References](#)[Tables](#)[Figures](#)[◀](#)[▶](#)[◀](#)[▶](#)[Back](#)[Close](#)[Full Screen / Esc](#)[Printer-friendly Version](#)[Interactive Discussion](#)

Air-snow transfer of nitrate in East Antarctica – Part 1

J. Erbland et al.

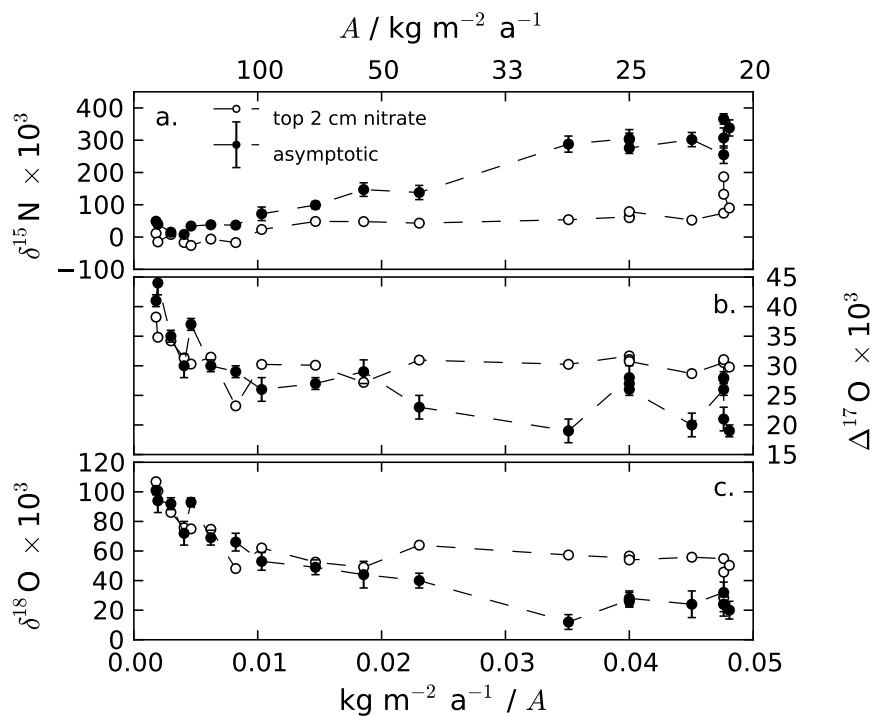


Fig. 13. Asymptotic nitrate isotopic composition and the isotopic composition of nitrate in the top 2 cm of snow in East Antarctica. **(a)** $\delta^{15}\text{N}(\text{NO}_3^-)$, **(b)** $\Delta^{17}\text{O}(\text{NO}_3^-)$ and **(c)** $\delta^{18}\text{O}(\text{NO}_3^-)$.

Title Page

Abstract

Introduction

Conclusions

References

Tables

Figures

◀

▶

◀

▶

Back

Close

Full Screen / Esc

Printer-friendly Version

Interactive Discussion

